nature medicine

Article

https://doi.org/10.1038/s41591-024-02851-9

A shared neoantigen vaccine combined with immune checkpoint blockade for advanced metastatic solid tumors: phase 1 trial interim results

Received: 11 October 2023

Accepted: 29 January 2024

Published online: 27 March 2024

Check for updates

A list of authors and their affiliations appears at the end of the paper

Therapeutic vaccines that elicit cytotoxic T cell responses targeting tumor-specific neoantigens hold promise for providing long-term clinical benefit to patients with cancer. Here we evaluated safety and tolerability of a therapeutic vaccine encoding 20 shared neoantigens derived from selected common oncogenic driver mutations as primary endpoints in an ongoing phase 1/2 study in patients with advanced/metastatic solid tumors. Secondary endpoints included immunogenicity, overall response rate, progression-free survival and overall survival. Eligible patients were selected if their tumors expressed one of the human leukocyte antigen-matched tumor mutations included in the vaccine, with the majority of patients (18/19) harboring a mutation in *KRAS*. The vaccine regimen, consisting of a chimp adenovirus (ChAd68) and self-amplifying mRNA (samRNA) in combination with the immune checkpoint inhibitors ipilimumab and nivolumab, was shown to be well tolerated, with observed treatment-related adverse events consistent with acute inflammation expected with viral vector-based vaccines and immune checkpoint blockade, the majority grade 1/2. Two patients experienced grade 3/4 serious treatment-related adverse events that were also dose-limiting toxicities. The overall response rate was 0%, and median progression-free survival and overall survival were 1.9 months and 7.9 months, respectively. T cell responses were biased toward human leukocyte antigen-matched TP53 neoantigens encoded in the vaccine relative to KRAS neoantigens expressed by the patients' tumors, indicating a previously unknown hierarchy of neoantigen immunodominance that may impact the therapeutic efficacy of multiepitope shared neoantigen vaccines. These data led to the development of an optimized vaccine exclusively targeting KRAS-derived neoantigens that is being evaluated in a subset of patients in phase 2 of the clinical study. ClinicalTrials.gov registration: NCT03953235.

Immunotherapies that harness the immune system to target tumor cells have shown considerable clinical benefit in a wide range of tumor types, though are generally limited to a subset of patients. The therapeutic benefit provided by immune checkpoint blockade (ICB) correlates with the presence of preexisting, tumor-infiltrating neoantigen-specific $CD8^+$ T cells that recognize and kill tumor cells[1,2]. These highly immunogenic neoantigens hold promise as targets for therapeutic vaccines, designed to activate and expand tumor-specific T cell responses.

e-mail: kjooss@gritstone.com

A previous study demonstrated that an individualized, heterologous prime-boost vaccine regimen, consisting of chimpanzee adenovirus (ChAd68) and self-amplifying mRNA (samRNA) delivering 20 patient-specific neoepitopes in combination with nivolumab and ipilimumab, induces potent, polyfunctional, neoantigen-specific $CD8^+$ T cell responses in patients with advanced stage, metastatic tumors[3]. In contrast to individualized neoantigen vaccines, vaccines targeting shared neoantigens identified from common oncogenic driver mutations, such as those in *KRAS* or *TP53*, provide the opportunity for 'off-the-shelf' vaccines that circumvent the need for individualized vaccine manufacture.

Targeting *KRAS* mutations is a promising therapeutic approach, as *KRAS* is the most frequently mutated oncogene in human cancer, occurring in more than 80% of pancreatic cancers and 50% of colorectal cancers (CRCs), as well as 30% of lung adenocarcinomas[4]. Small molecule inhibitors of KRAS G12C mutation have provided clear clinical benefit[5–8]; however, acquired resistance mutations are observed within months of treatment[9,10]. As an alternative, therapeutic vaccines eliciting T cell responses specific for KRAS mutations may offer more durable clinical benefit to patients with *KRAS* mutation-carrying solid tumors, and both treatment approaches could be combined to enhance overall antitumor efficacy.

In this Article, we report interim results from the phase 1 portion of the phase 1/2 clinical trial (NCT03953235) assessing safety, tolerability, preliminary clinical activity and immunogenicity of an off-the-shelf vaccine (SLATEv1) utilizing the heterologous ChAd68/samRNA-based vaccine regimen in combination with nivolumab and ipilimumab described previously[3] but encoding 20 shared neoantigens targeting recurrent mutations in several oncogenes, including *KRAS* and *TP53*. These neoantigens were identified using EDGE, a previously described class I epitope prediction model[11], and selected on the basis of the frequency of presentation of these neoantigens by human leukocyte antigen (HLA) class I alleles in patient populations with solid tumors. As vaccine-induced T cells can express programmed cell death protein 1 (PD-1), which can inhibit their effector function, all patients received concurrent nivolumab to maintain T cell function in the tumor microenvironment[12]. All patients received the same dose of ChAd68 with escalating doses of samRNA in four dose levels (DLs), with ipilimumab being administered at DLs 2–4. Ipilimumab was administered subcutaneously (SC) in proximity of the vaccine draining lymph nodes, to increase anti-CTLA-4 concentration where vaccine-induced T cell activation occurs and enhance the breadth and magnitude of the T cell response[3]. As ipilimumab was administered via a novel route of administration, inclusion in DLs 2–4 enabled assessment of the safety of combining ipilimumab with the vaccine and nivolumab compared to DL 1. Patients enrolled in this study had solid tumors harboring one of the 20 neoantigens encoded by the vaccine cassette and an HLA class I allele validated or predicted to present the patient-specific neoantigen. Primary endpoints of the phase 1 part of the study were safety and tolerability and initial recommended phase 2 dose (RP2D). Secondary endpoints included immunogenicity, overall response rate (ORR) based on the best overall response (BOR), clinical benefit rate (CBR), progression-free survival (PFS) and overall survival (OS). Changes in circulating tumor DNA (ctDNA) in blood were assessed as an exploratory endpoint. Analysis of T cell responses in patients suggested a hierarchy of neoantigen immunodominance, which was explored preclinically using mass spectrometry (MS) analysis in cell lines and HLA-transgenic mice, leading to the development of a second-generation shared neoantigen vaccine encoding an optimized neoantigen cassette targeting four KRAS-derived neoantigens (SLATE–KRAS).

Results

Design of shared neoantigen vaccine

A shared neoantigen-specific vaccine (SLATEv1) was designed to encode 20 neoantigens derived from recurrent oncogenic driver mutations (Extended Data Table 1). The selected neoantigens included epitopes that were validated by detection via MS of a neoepitope peptide arising from the mutated sequence in either patient tumors or monoallelic HLA-expressing engineered cell lines (Supplementary Data) or previously published[13]. Additional neoantigens were included that were predicted to have a high probability of presentation on the tumor cell surface using EDGE, a proprietary antigen prediction neural network model[11]. The included mutations along with their associated HLA alleles (Extended Data Table 1) are estimated to occur in approximately 10–17% of patients with non-small cell lung cancer (NSCLC), CRC and pancreatic ductal adenocarcinoma (PDA) at similar distributions across racial groups[14–17]. The SLATEv1 neoantigen vaccine regimen was evaluated in a first-in-human phase 1/2 study in patients whose tumors harbor one of the encoded neoantigens and a matched HLA allele.

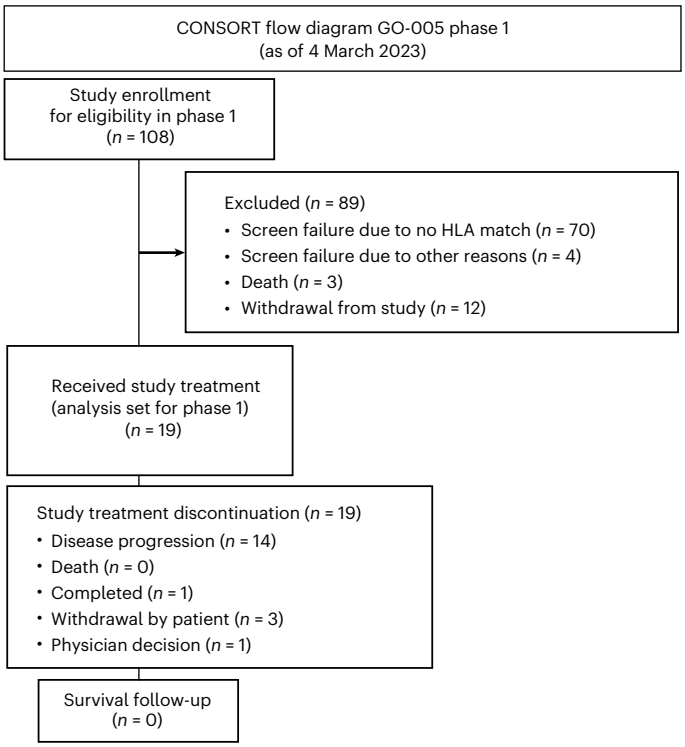

Fig. 1 | CONSORT diagram. CONSORT flow diagram of patient enrollment.

Shared neoantigen vaccine regimen is well tolerated

Nineteen patients with previously treated metastatic cancer were treated in the phase 1 portion of this study (Fig. 1). The majority of patients were female (12/19, 63.2%) and had an Eastern Cooperative Oncology Group (ECOG) score of 1 (16/19, 84.2%) with the remaining three patients having an ECOG score of 0 (Table 1). The median age was 61 years (range 33–83 years). Tumor types included patients with NSCLC (6/19, 31.6%), CRC (6/19, 31.6%), PDA (5/19, 26.3%), pancreatobiliary adenocarcinoma (1/19, 5.3%) and ovarian cancer (1/19, 5.3%). The median time to vaccination with SLATEv1 from first cancer diagnosis was 25.9 months, and all patients received one (10/19, 52.6%) or more prior line(s) of therapy (9/19, 47.4%; Table 1 and Extended Data Table 2). All six patients with NSCLC received prior anti-PD-(L)1 therapy, with one patient also receiving an anti-TIGIT antibody. All patients had progressive disease (PD) at the time of treatment initiation. The phase 1 portion of the study evaluated four DLs with dose escalation of samRNA boost vaccination based on a modified toxicity probability interval 2 (mTPI-2) design[18,19] (Fig. 2a). There was no dose escalation of the ChAd68 dose, and three different samRNA boost vaccination doses were evaluated in combination with SC ipilimumab (30 mg) at DLs 2–4. All patients

https://doi.org/10.1038/s41591-024-02851-9

Table 1 | Baseline and disease characteristics by DL

	DL 1	DL 2	DL 3	DL 4	Total
	(*n*=2)	(*n*=4)	(*n*=6)	(*n*=7)	(*n*=19)
Age (year),	75	65.5	61	54	61
median (range)	(67–83)	(33–78)	(48–75)	(35–79)	(33–83)
Female gender, *n* (%)	1 (50)	1 (25)	5 (83)	5 (71)	12 (63)
ECOG, *n* (%)					
0	0 (0)	1 (25)	1 (17)	1 (14)	3 (16)
1	2 (100)	3 (75)	5 (83)	6 (86)	16 (84)
Number of prior therapies, *n* (%)					
1	0 (0)	3 (75)	3 (50)	4 (57)	10 (53)
2	0 (0)	1 (25)	1 (17)	1 (14)	3 (16)
3	2 (100)	0 (0)	2 (33)	2 (29)	6 (32)
Prior anti-PD(L)1 therapy, *n* (%)					
Yes	2 (100)	2 (50)	1 (17)	1 (14)	6 (32)
No	0 (0)	2 (50)	5 (83)	6 (86)	13 (68)
Tumor types, *n* (%)					
CRC	0 (0)	1 (25)	2 (33)	3 (43)	6 (32)
NCSLC	2 (100)	2 (50)	1 (17)	1 (14)	6 (32)
PDA	0 (0)	1 (25)	2 (33)	2 (29)	5 (26)
Ovarian adenocarcinoma	0 (0)	0 (0)	1 (17)	0 (0)	1 (5)
Pancreatobiliary adenocarcinoma	0 (0)	0 (0)	0 (0)	1 (14)	1 (5)

DL 1, GRT-C903/GRT-R904 30 µg + nivolumab; DL 2, GRT-C903/GRT-R904 30 µg + nivolumab + SC ipilimumab; DL 3, GRT-C903/GRT-R904 100 µg + nivolumab + SC ipilimumab; DL 4, GRT-C903/GRT-R904 300 µg + nivolumab + SC ipilimumab

received concurrent nivolumab (480 mg) administered intravenously every 4 weeks.

A primary endpoint of the phase 1 portion of the study was the safety and tolerability of a prime vaccination with ChAd68 followed by repeated boost vaccinations with the samRNA vaccine (Fig. 2b), both administered intramuscularly (IM). Overall, the vaccine regimen was well tolerated, with the most common treatment-related adverse events (TRAEs) being pyrexia, fatigue, nausea, vomiting and diarrhea, all of which were grade 1/2 except for one TRAE of grade 3 fatigue (Table 2 and Supplementary Data Table 1). The majority of TRAEs were self-limiting and resolved with either antipyretics or without intervention. Two patients had treatment-related serious adverse events (SAEs) consistent with those previously observed with ICB[20] (Table 2). One patient had liver enzyme elevation (grade 4 aspartate aminotransferase elevation and grade 3 alanine transaminase elevation) and pyrexia after ChAd68 that resolved with steroids and antipyretics, as well as grade 3 decreased neutrophil count after samRNA that resolved without intervention, and one patient had grade 3 rhabdomyolysis that resolved with steroids. None of the patients discontinued study treatment due to a TRAE. The primary reason for study treatment discontinuation was disease progression (14/19 patients), followed by withdrawal by patient (3/19), physician decision (1/19) or treatment completion (1/19; Fig. 1 and Extended Data Table 2).

Patients were evaluated for dose-limiting toxicities (DLTs) for 28 days following the ChAd68 prime and 28 days following the first samRNA boost. Two patients experienced a DLT after receiving ChAd68 in combination with nivolumab and ipilimumab (Table 2). These 2 patients received the same dose of ChAd68 in combination with nivolumab and ipilimumab as 15 additional patients treated at DLs 2–4 who did not experience a DLT. Thus, the observed DLTs did not result in a dose modification. No DLTs were observed in patients treated with ChAd68 and only nivolumab (DL 1, $n = 2$), and no DLTs were observed following treatment with samRNA across all DLs. Overall, the ChAd68/samRNA vaccine regimen in combination with SC ipilimumab and intravenous nivolumab was demonstrated to be well tolerated at all DLs. Based on the totality of the safety and immunogenicity (secondary endpoint, see 'Effective tumor growth control in subset of treated patients' section) data from the phase 1 portion of the study, and the final RP2D was determined to be 10^{12} viral particles (VPs) ChAd68 and 30 µg samRNA. There were no protocol amendments during the enrollment for the phase 1 of this study.

Effective tumor growth control in subset of treated patients

The clinical activity of the vaccine regimen was evaluated via the secondary endpoints of the phase 1 study, ORR and PFS, as assessed by RECIST v1.1 criteria and OS. A total of 8 out of 19 patients (42%) had a BOR of stable disease (Fig. 2c and Extended Data Table 2), with 3 patients demonstrating decreases in target lesions (Extended Data Fig. 1). A total of 11 of 19 patients had a BOR of PD. The CBR was 42%, and since there were no confirmed ORs, there was no assessment of duration or deepening of response. The median PFS for all phase 1 patients was 1.9 months (95% confidence interval (CI) 1.7–3.9 months). The median OS across all tumor types was 7.9 months (95% CI 4.7–10.9 months). A total of 79% of patients (15/19) treated in phase 1 experienced PD, with all progressing early in the treatment course, when the neoantigen-specific T cell response is still being generated (11/15 within 2 months and 4/15 within 4 months after the first vaccination).

Anticancer activity with immunotherapies that induce robust T cell responses may be miscategorized by radiography due to T cell infiltration into the tumor that may lead to increases in tumor size. The monitoring of ctDNA in blood has been shown to correlate with clinical outcomes[21–23] and may be a more sensitive marker of treatment effects with immunotherapy compared to computed tomography scans[24]. Therefore, the level of ctDNA corresponding to the targeted neoantigen within the vaccine cassette was assessed as an exploratory endpoint. A molecular response (MR) characterized by a ≥30% reduction in neoantigen-specific ctDNA compared to baseline levels was observed in 33% of patients evaluable for MR (4/12; Fig. 2d). In addition to a reduction in the ctDNA level of the vaccine targeted neoantigen, a decrease in ctDNA for additional variants not encoded by the vaccine (selected from a panel of common driver mutations) was observed in all four patients with an MR (Extended Data Fig. 2), providing evidence for effective tumor targeting.

One mechanism through which tumors evade immune control is through disruption of antigen presentation. An immune evasion panel was included in the ctDNA analysis to assess whether patients demonstrated defects in antigen presentation upon progression. Two patients, one an MR and the other a molecular nonresponder, demonstrated progressive loss-of-heterozygosity (LOH) of the relevant neoantigen matched *HLA* allele over the course of treatment (Extended Data Fig. 3), suggesting that vaccine-induced T cells exerted immune pressure on the tumor, triggering this immune escape mechanism. One of the molecular responders, S13, showed evidence of *HLA* LOH ($P = 0.015$) in the baseline sample, which was not evident in a post-treatment sample corresponding with the drop in ctDNA but was observed at all subsequent time points ($P < 0.01$) and was associated with PD, suggesting the outgrowth of tumor cells resistant to T cell control (Extended Data Fig. 3b). The other patient, S4, had a variant resulting in the loss of the *B2M* start codon, which has been shown to reduce antigen presentation[25,26], detected at low frequency at baseline and increasing in frequency during treatment with the vaccine regimen (Extended Data Fig. 2e), as well as complete *HLA* LOH at the final collected time point (Extended Data Fig. 3c). The *B2M* mutation and complete LOH may explain the lack of clinical activity observed in this patient.

https://doi.org/10.1038/s41591-024-02851-9

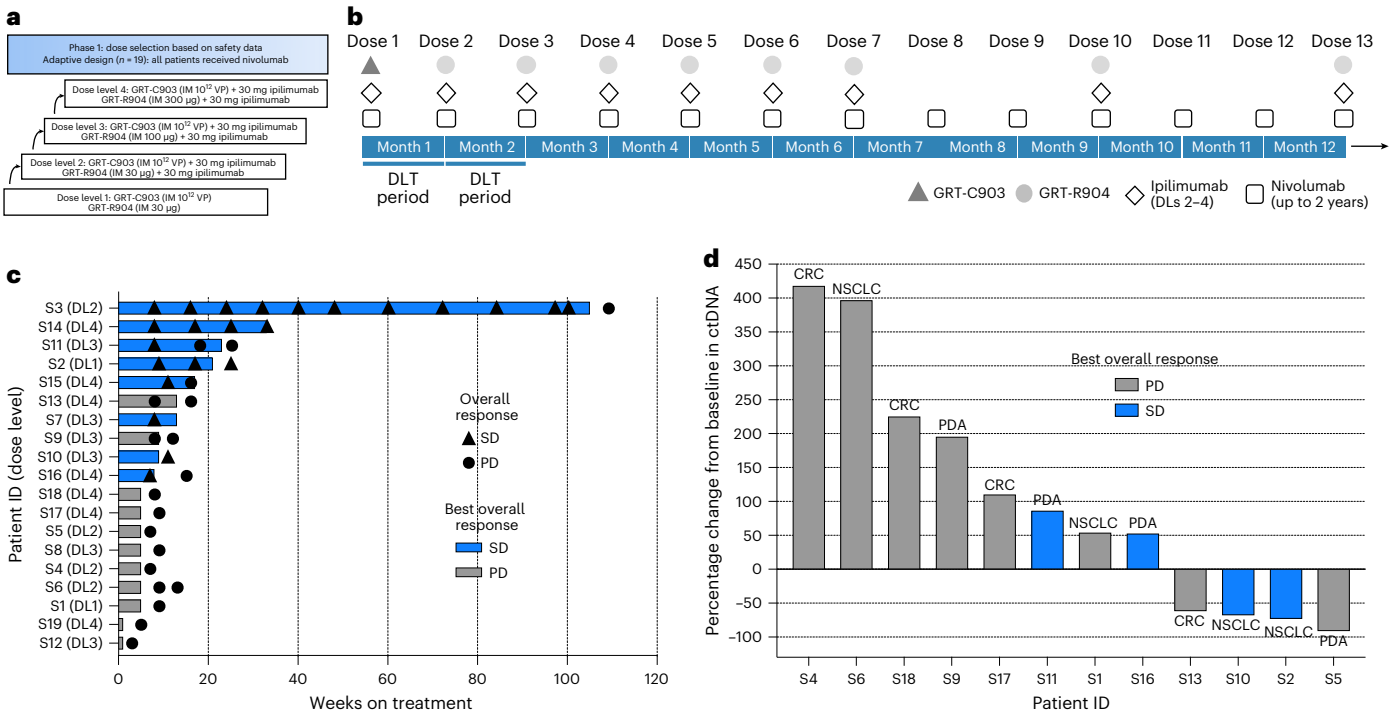

Fig. 2 | Data from the phase 1 portion of trial show the vaccine regimen is well tolerated and leads to stable disease and/or MR in a subset of patients. **a**, A phase 1 study schematic outlining dose escalation. **b**, A phase 1 treatment regimen. **c**, A swimmer plot of phase 1 patients ($n = 19$) treated with SLATE v1. RECIST response at each time point depicted, length of bars represent time on treatment. **d**, The best percent change in ctDNA following initiation of study treatment relative to baseline levels colored by best overall RECIST-based response. The tumor type is annotated, and $n = 12$. Seven patients with no detectable baseline ctDNA level were excluded.

Table 2 | Summary safety data across all treated patients

	Grade 1/2	Grade 3/4
	n[a] (%)	*n*[a] (%)
TRAE >10%		
Pyrexia	11 (58)	0
Fatigue	6 (32)	1 (5)
Nausea	5 (26)	0
Vomiting	5 (26)	0
Diarrhea	4 (21)	0
Chills	3 (16)	0
Pruritus	3 (16)	0
Asthenia	2 (11)	0
Dizziness	2 (11)	0
Injection site pain	2 (11)	0
Injection site reaction	2 (11)	0
Myalgia	2 (11)	0
Treatment-related SAE >5%		
Pyrexia	1 (5)	0
Rhabdomyolysis[b]	0	1 (5)
Alanine aminotransferase increased[c]	0	1 (5)
Aspartate aminotransferase increased[c]	0	1 (5)
Neutrophil count decreased	0	1 (5)

[a]Number of patients that experienced reported AE. If a patient experienced multiple AEs of same preferred term, the highest grade AE was counted. Percent is out of total treated patients ($n = 19$). [b]DLT following GRT-C901, patient S19 (DL4). [c]DLT following GRT-C901, patient S16 (DL4).

Vaccine induces T cell responses to dominant TP53 antigens

To further investigate the mechanisms underlying the observed clinical activity, neoantigen-specific T cell responses were assessed as a secondary endpoint at various time points in peripheral blood mononuclear cells (PBMCs) in 18/19 patients, all of whom harbored *KRAS* mutations (Extended Data Table 2). T cell responses to the HLA-matched KRAS neoantigen expressed by the patients' tumors were measured by ex vivo IFNγ ELISpot in samples from 16 patients, and positive responses were observed in 31% (5/16) of patients at one or more postvaccination time point(s) (Fig. 3a and Extended Data Fig. 4). Within this subset, strong responses (>400 spot-forming units (SFU)/10^6 PBMCs) were detected in three patients, and responses in four patients increased over levels observed pretreatment. For two patients with positive KRAS responses for whom longitudinal samples were collected, KRAS-specific T cell responses were durable for up to 6 months post-ChAd68 prime (Extended Data Fig. 4). To determine if antigen-specific T cells were present at frequencies below the limit of detection (LOD) for the ex vivo ELISpot assay, in vitro stimulation (IVS), followed by IFNγ ELISpot, was performed on samples from 17 patients (Fig. 3b). After antigen-specific T cell expansion, 88% (15/17) of patients had detectable T cell responses to their HLA-matched tumor-specific KRAS neoantigen at a postvaccination time point. For those patients with positive KRAS responses post-treatment that were also assessed for preexisting T cell responses at baseline (1 patient not tested due to limited sample), treatment with SLATEv1 led to de novo priming of T cells in 29% (4/14) of patients, while responses were either maintained or boosted in 71% (10/14) of patients.

In addition to T cell responses specific to the tumor-relevant neoepitope, responses to other vaccine-encoded neoantigens were assessed that were validated to be presented by the same class I allele as the tumor-matched neoepitope (but were not expressed by the patient's tumor). Notably, ex vivo T cell responses to tumor-irrelevant

https://doi.org/10.1038/s41591-024-02851-9

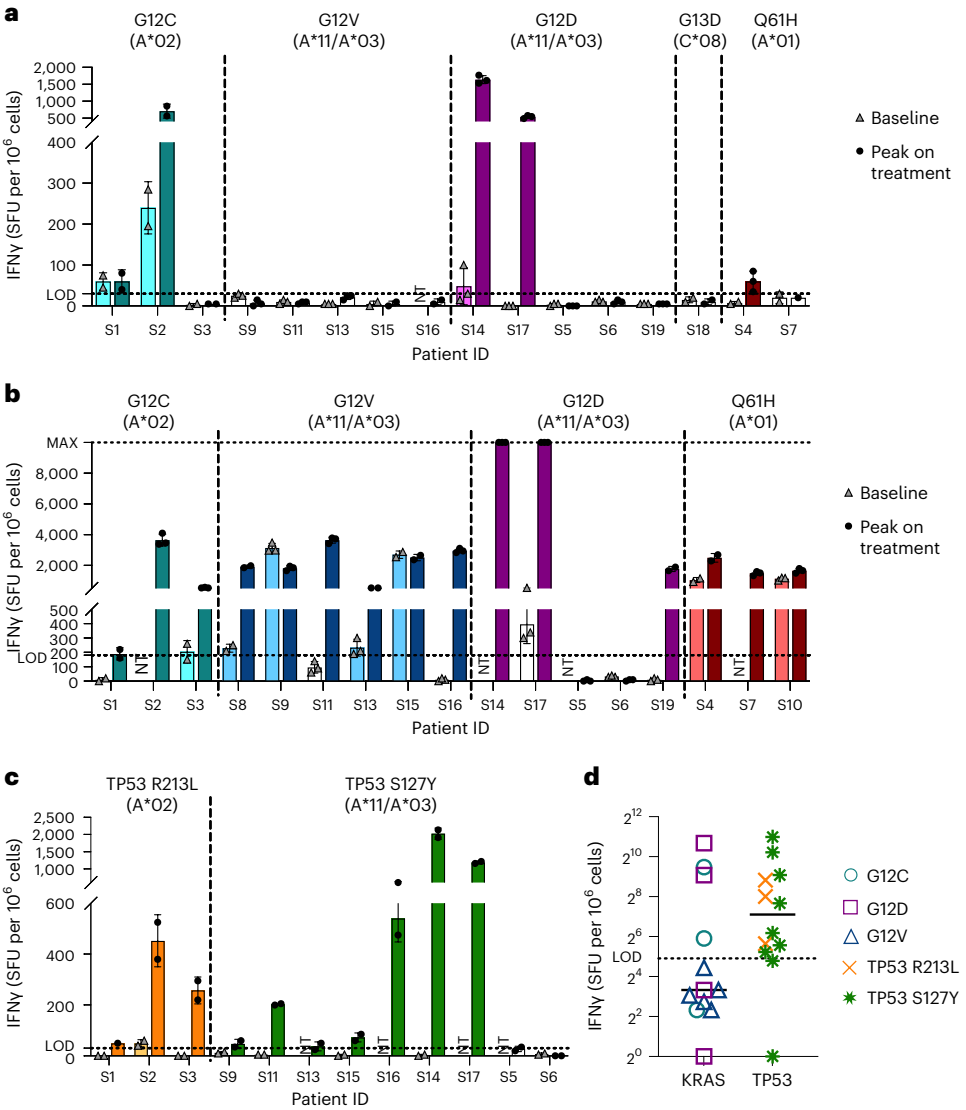

Fig. 3 | Immunogenicity data from patients enrolled in the phase 1 trial. **a**, Antigen-specific T cell responses to patient tumor antigen measured by ex vivo IFNγ ELISpot in PBMCs at baseline and at peak response postvaccination for each patient ($n = 16$, and patients S8 and S10 were not tested by ex vivo ELISpot; LOD 30). **b**, T cell responses to KRAS antigens measured by IFNγ ELISpot following IVS expansion ($n = 17$, and patient S18 was not tested; LOD 180). **c**, TP53 responses assessed by ex vivo IFNγ ELISpot (the peak response postvaccination is shown). TP53 mutation responses were measured for each patient with an HLA allele capable of presenting both the tumor-relevant KRAS epitope and the tumor-irrelevant TP53 epitopes ($n = 12$, and patients S8 and S19 were not tested). Patients S4, S7, S10 and S18 have no HLA match to TP53; LOD 30). The mean ± s.d. of two or three replicate wells (**a**–**c**). NT, not tested. The filled bars are positive responses and the empty bars are negative responses. For samples with unstimulated negative control (DMSO) values less than the LOD, positive values are defined as mean SFU > LOD. For two samples where the DMSO value was greater than the LOD, positive values are defined as mean SFU >2× the average DMSO value. Phytohemagglutinin positive control was assessed for each sample. **d**, Summary of KRAS and TP53 ex vivo ELISpot responses in A*02:01, A*03:01 or A*11:01 patients vaccinated with SLATEv1, $n = 12$ (patients S8 and S19 were not tested for both mutations). The horizontal dashed lines indicate the median (LOD 30).

TP53 neoepitopes were observed in 83% (10/12) of patients with an *HLA* allele capable of presenting both the tumor-relevant KRAS epitope and the tumor-irrelevant TP53 epitopes (Fig. 3c, four patients excluded due to lack of relevant *HLA* and two patients were excluded due to limited sample availability). TP53 responses were observed more frequently via ex vivo ELISpot than KRAS responses within this patient subset (83% compared to 33%, Fig. 3d), suggesting potential immune competition between the delivered antigens.

Optimization for KRAS presentation and immune response

To assess the role of epitope processing and presentation on potential immune hierarchy, the target densities of KRAS and TP53 neoantigens in vitro were assessed by MS in HLA-A*11:01 monoallelic cell lines expressing selected vaccine cassettes (Fig. 4a). The inclusion of a stable isotope-labeled (heavy) peptide HLA complex matching each neoantigen target enabled correction for processing loss and more accurate comparisons of copy number. Cassette expression, as determined by reverse-transcription polymerase chain reaction (RT–qPCR; Extended Data Fig. 5), was used to normalize copy number, as variation of expression can influence efficiency of antigen presentation. Expression of the SLATEv1 vaccine cassette (20×1) elicited antigen presentation for KRAS G12V, KRAS G12D, KRAS G12C and TP53-S127Y epitopes predicted to be presented by HLA-A*11:01 (Fig. 4b). Interestingly, expression of a KRAS-focused cassette encoding only four KRAS neoantigens (4×1) led to an approximately threefold increase in target density of all three KRAS neoantigens, compared to SLATEv1 (20×1; Fig. 4b). The addition of either TP53 epitope to the KRAS 4×1 cassette (4×1-R213L, 4×1-S127Y) led to an approximately twofold reduction

https://doi.org/10.1038/s41591-024-02851-9

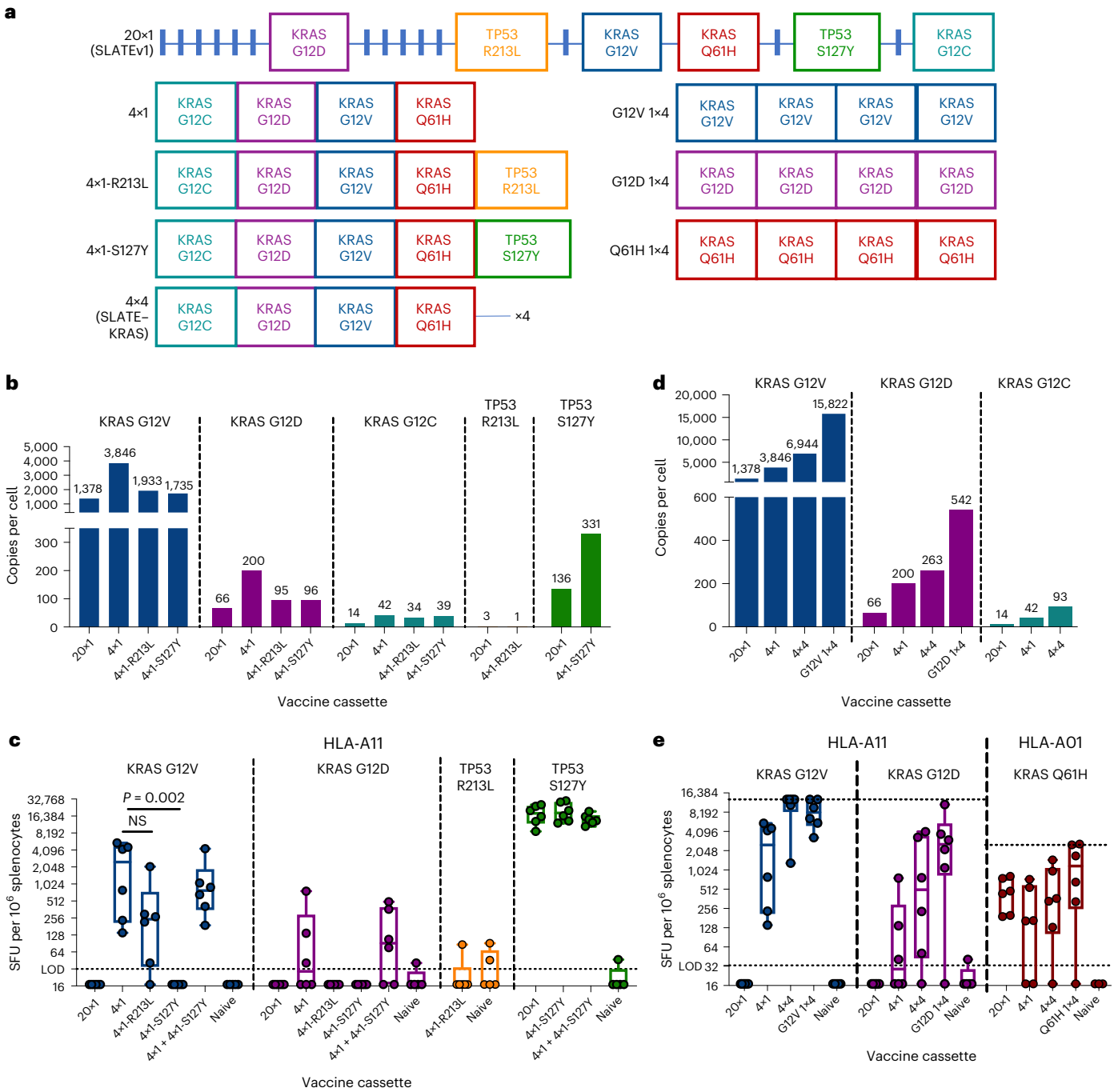

Fig. 4 | Removal of immunodominant epitopes and repetition of epitopes leads to increased target density and T cell response to KRAS mutant neoantigens. a, Design of vaccine epitope cassettes evaluated for target density in human HLA-A*11:01 monoallelic cell lines and HLA-transgenic mice. The boxes depict antigens that were assessed for the corresponding HLA-restricted peptide presentations by MS and immunogenicity, and the lines represent other epitopes that were not measured. **b**,**d**, Endogenous neoantigen target density quantified using internal heavy standard peptide HLA complexes added to lysates of K562 cells transduced with lentiviral vectors of HLA-A*11:01 and constructs indicated in **a**. The peptides reported as copies/cell normalized to cassette expression measured by RT–qPCR (Extended Data Fig. 5). All samples were processed in one experiment. Cassettes with one copy of each epitope shown in **b**, comparison to cassettes with epitopes repeated 4 times in **d**. **c**,**e**, Antigen-specific T cell response assessed in splenocytes of specified HLA transgenic mice 2 weeks postimmunization with the specified ChAd68 vaccine (5×10^{10} VP each) by IFNγ ELISpot following overnight stimulation with the specified peptide pool containing all possible 8–11mer epitopes spanning the neoantigen 25mer. The background (mean value for DMSO negative control) was subtracted for each sample ($n = 6$ mice per group). The box and whiskers represent interquartile range (IQR) and range and the horizontal line is the median on a $\log_2$ scale (LOD 33, values <LOD set to one-half LOD). In **e**, the samples that were too numerous to count were set to an assay maximum (MAX of 13,000 SFU/10^6 for HLA-A11 experiment and 2,600 SFU/10^6 for HLA-A*01 experiment). The data are representative of two repeat studies for HLA-A*11 data (two-tailed Mann–Whitney). NS, not significant. Cassettes with one copy of each epitope shown in **c**, comparison to cassettes with epitopes repeated 4 times in **e**.

in target density of the KRAS G12D and KRAS G12V epitopes compared to the 4×1 cassette (Fig. 4b). The negative impact of the additional TP53 epitope on KRAS neoantigen presentation was observed with both the HLA-matched S127Y epitope, which is presented at high levels by HLA-A*11:01 (Fig. 4b) and with the HLA-irrelevant R213L epitope, which is presented at high levels in the context of HLA-A*02:01 but not HLA-A*11:01 (Extended Data Fig. 5c). Therefore, while the observed decrease in KRAS neoantigen presentation may be partially a result of competition for major histocompatibility complex binding by immune dominant epitopes, additional features of cassette sequence, design and expression may also impact antigen presentation. Although KRAS G12C target density was detectable in all cell lines, presentation by HLA-A*11:01 was low overall.

To assess the impact of potentially immunodominant TP53 epitopes on the immune response to KRAS neoantigens, ChAd68 vaccines encoding the same neoantigen cassettes used for the generation of cell lines assessed by MS (Fig. 4a) were evaluated for immunogenicity in HLA-A*11:01 transgenic mice. Consistent with the observed immune response patterns in patients, a ChAd68 vaccine encoding the SLATEv1 cassette (20×1) induced potent T cell responses to the HLA-A*11:01-matched TP53-S127Y neoantigen in mice (GeoMean 17,003 SFU/10^6 splenocytes), while no response was detected to the KRAS-G12V or G12D neoantigens (6/6 mice <LOD, Fig. 4c). In contrast, a KRAS-focused cassette (4×1) induced a strong T cell response to the KRAS-G12V neoantigen (GeoMean 1,185 SFU/10^6 splenocytes, Fig. 3c). A low and inconsistent response was observed across animals to the KRAS G12D neoantigen (Fig. 4c), while low or no response was detected to KRAS G12C neoantigen (Extended Data Fig. 6a), consistent with the low target density observed in HLA-A*11:01 cell lines via MS (Fig. 4b). These results suggest a threshold of antigen expression and presentation required for vaccine-induced T cell responses in transgenic mice. Consistent with the antigen presentation data (Fig. 4b), the addition of either the HLA-matched TP53-S127Y neoantigen or the HLA-irrelevant TP53-R213L to the KRAS-focused cassette (4×1-S127Y, 4×1-R213L) led to reduced T cell responses to KRAS-G12V and G12D. Interestingly, while the addition of TP53-R213L, which drives a strong T cell response in HLA-A*02:01 mice (Extended Data Fig. 6b) and no response in HLA-A*11:01 mice (Fig. 4c), led to a 6.2-fold decrease in T cell response to KRAS-G12V (Fig. 3c). The addition of TP53-S127Y, which elicited strong TP53-S127Y-specific T cell responses (GeoMean 19,174 SFU/10^6 splenocytes), completely eliminated T cell responses to the KRAS-G12V neoantigen (6/6 mice <LOD, Fig. 4c). Notably, all the vaccines assessed in transgenic mice elicited a similar magnitude of T cell responses to a universal (Pan-DR) class II antigen located at the carboxy terminus of the vaccine cassettes, suggesting observed differences in antigen-specific $CD8^+$ T cell responses are not a result of variable expression of the vaccine cassettes (Extended Data Fig. 6c,d). These results implicate additional processes beyond antigen presentation that play a role in immune response hierarchies in vivo and suggest that the lack of observed T cell responses to the KRAS-G12V neoantigen elicited by the SLATEv1 (20×1) vaccine is due to an immunodominant response to TP53-S127Y, which is presented by the same HLA molecule. To overcome the observed immune competition, the KRAS-G12V and the TP53-S127Y neoantigens were delivered in two different vaccine vectors, injected bilaterally into separate muscles in mice (4×1+4×1-S127Y), which led to strong T cell responses to both the TP53-S127Y and KRAS-G12V neoantigens (GeoMean 14,240 and 775 SFU/10^6 splenocytes, Fig. 3c). Similar results were observed using mouse-specific H2-Kd restricted tumor antigens in Balb/c mice, with the inclusion of a dominant antigen suppressing the immune response to a subdominant antigen when expressed by the same ChAd68 vaccine cassette, which was rescued by expression of each antigen on separate vaccine vectors, either delivered via two separate injections or blended in the same syringe (Extended Data Fig. 7). These data suggest that immune dominance can occur when antigens are expressed from the same vaccine cassette in the same target cell and can be rescued by delivering the antigens to different target cells, which is achieved by delivering them via separate vaccine vectors, consistent with previous studies using DNA vaccines[27].

Neoantigen repetition increases presentation and T cell response

To further enhance the immunogenicity of the SLATE vaccine to the immune subdominant KRAS-derived neoantigens, we encoded multiple repeats of each neoantigen within the same vaccine cassette. We previously observed increased T cell responses to multiple different mouse-specific tumor antigens when they were repeated within the vaccine cassette, with increasing T cell response correlating to the number of repeats (Extended Data Fig. 8). Cell lines expressing three additional cassettes (Fig. 4a) were compared by MS: KRAS-G12V 1×4, KRAS-G12D 1×4 and 4×4 (or 'SLATE–KRAS', which includes four repeats each of KRAS G12V, G12D, G12C and Q61H). The results showed that repeating epitopes increased target density for all three KRAS epitopes: G12V, G12D and G12C (Fig. 4d). The increase in target density was moderate (~1.3- to 2-fold) in the 4×4 cassette, which harbors all four KRAS epitopes repeated four times, but even greater (~3- to 4-fold), for 1×4 cassettes that have no competing epitopes. Consistent with this observation, a vaccine encoding four repeats of each KRAS neoantigen (4×4) drove significantly increased T cell responses to KRAS G12V compared to the vaccine cassette encoding only one copy (4×4 versus 4×1, Fig. 4e; $P = 0.013$, two-tailed Mann–Whitney). Increased T cell responses were also observed to the KRAS G12D neoantigen in HLA-A*11:01 mice, as well as the KRAS Q61H neoantigen in HLA-A*01:01 mice (Fig. 4e). A KRAS G12V-specific vaccine cassette, encoding only the KRAS G12V neoantigen repeated four times (G12V 1×4), also led to increased G12V-specific T cell responses compared to the 4×1 cassette, with similar T cell responses as the 4×4, suggesting that the increased response is driven by the repetition of the neoantigen (Fig. 4e). Similarly, increased T cell responses were observed with KRAS G12D- and KRAS Q61H-specific vaccine cassettes (G12D 1×4 and Q61H 1×4) compared to the 4×1 and were slightly increased when compared to the 4×4 (Fig. 4e). These data demonstrate enhanced antigen presentation and T cell responses to KRAS neoantigens utilizing a KRAS-focused vaccine cassette incorporating repetition of four highly prevalent KRAS epitopes (SLATE–KRAS) when compared to a version 1 vaccine cassette (SLATEv1) that consisted of one copy each of 20 different neoepitopes.

Discussion

An 'off-the-shelf' shared neoantigen vaccine, consisting of ChAd68 and samRNA vectors in combination with ICB, was assessed in patients with advanced/metastatic solid tumors. The vaccine (SLATEv1) encoded 20 shared neoantigens derived from selected common oncogenic driver mutations, which were identified using EDGE, a proprietary epitope prediction model[11] validated for antigen presentation via MS, or previously published[13]. In contrast to prior off-the-shelf vaccines targeting KRAS[28], patients with an HLA-matched tumor mutation included in the vaccine were selected, as patients who do not have an HLA allele that can present the neoepitope on the tumor cell surface are not expected to benefit from this approach. The vaccine regimen was shown to be well tolerated, with observed TRAEs consistent with acute inflammation expected with viral-based vaccine vectors[29–31] and ICB[20]. Preliminary signals of clinical activity were observed with disease stabilization associated with tumor shrinkage and MR in some patients.

Despite some evidence of clinical benefit, disease progression was observed in 15/19 patients, most of whom progressed within the first 2 months following vaccination, probably before mounting a sufficiently strong T cell response to halt disease progression. The median OS was less than 8 months, evidence of the very advanced nature of the cancer in subjects studied, in whom active immunotherapy is least

likely to have sufficient time to establish disease control. This short time on study, in addition to restrictions on elective procedures due to the coronavirus disease 2019 pandemic, limited the availability of samples for analysis of immune responses in the periphery or the tumor. T cell responses specific to the SLATEv1 vaccine-encoded and tumor-relevant KRAS neoantigens were detected in 15/17 patients following antigen-specific in vitro expansion, demonstrating that the vaccine vectors can drive tumor-specific T cell responses. However, responses by ex vivo ELISpot were less frequent and lower in magnitude compared to previously observed results using the same vaccine vectors to deliver 20 individualized neoantigens (GRANITE), which led to potent antigen-specific ex vivo T cell responses to multiple neoantigens per patient[3]. Furthermore, while sample limitations and low antigen-specific responses prevented more extensive analysis in the current study, the previous study demonstrated vaccine-elicted polyfunctional, cytotoxic CD8 T cells, which were increased in the tumor following vaccination, as well as expanded neoantigen-specific effector memory T cells[3]. Interestingly, SLATEv1 vaccine-elicited T cell responses to HLA-matched. However, tumor-irrelevant, TP53 neoantigens were readily detected by ex vivo overnight ELISpot in 83% (10/12) of patients, while tumor-relevant KRAS neoantigens were only detected in 31% (5/16) of patients without in vitro antigen-specific T cell expansion. This result may reflect the lower immunogenicity of KRAS neoantigens and/or a possible hierarchy of immune dominance, in which strong immune responses to tumor-irrelevant neoantigens can suppress or outcompete T cell responses to subdominant neoantigens expressed by the tumor, limiting tumor control and clinical efficacy. This is consistent with studies demonstrating immunodominance hierarchies established during the antitumor immune response, as well as following microbial infections and vaccination, which may play a role in protective immunity for infectious disease and escape of immune control and tumor evolution in cancer[27,32,33]. To investigate this further, KRAS-focused neoantigen cassettes including only the top four highly prevalent KRAS neoantigens were generated and assessed preclinically for antigen presentation in cell lines by MS and immunogenicity in HLA-transgenic mice. Consistent with our hypothesis of immune competition, a KRAS-focused neoantigen cassette led to increased presentation of KRAS neoepitopes in cell lines and increased immune response to KRAS neoantigens in HLA-A*11 mice compared to the SLATEv1 cassette encoding 20 different neoantigens. Interestingly, this was not observed with an HLA-A*01-restricted KRAS neoantigen (Q61H) in HLA-A*01 mice, for which there were no other HLA-matched competing epitopes encoded within the SLATEv1 cassette. Furthermore, while the addition of either an HLA-matched or HLA-irrelevant TP53 neoantigen to the expression cassette led to similar reductions in KRAS epitope presentation, only the addition of the HLA-matched TP53 neoantigen led to complete loss of the KRAS-specific T cell response in mice, suggesting that antigen presentation is one, but not the only, factor determining immune dominance. For example, previous data in murine models have demonstrated that IFNγ expression by CD8 T cells specific to dominant epitopes may suppress the T cell response to subdominant epitopes[27]. Notably, this immune competition can be avoided by delivery of each antigen on separate vaccine vectors, probably due to expression in and presentation by different antigen-presenting cells (APCs). This is supported by studies demonstrating that coexpression of dominant and subdominant epitopes in the same APC is central to immunodominance[27,32]. This suggests that future vaccination approaches that aim to combine multiple shared neoantigens may be improved by combination of separate vaccine vectors to deliver antigens to different APCs and elicit broad T cell responses to both dominant and subdominant antigens, which may be needed to prevent tumor immune escape and recurrence[34] and to provide durable therapeutic benefit to patients.

The vaccine expression cassette was further optimized by the repetition of neoepitopes, which led to increased antigen presentation and immune response in transgenic mice. This was observed with multiple KRAS neoantigens across different HLAs, as well as with mouse tumor antigens, which demonstrated higher immune responses with increasing numbers of repeats. These observations have implications for the design of multiantigen vaccines, whereby the optimal immunogenicity may be achieved by blending of multiple vaccine vectors encoding repeats of each epitope.

In addition, the shared neoantigen vaccination approach used here, which encodes only a single tumor-matched neoantigen presented by a single HLA per patient, is more susceptible to immune escape mechanisms, such as *HLA* LOH, when compared to individualized vaccines such as GRANITE, which encode 20 tumor-specific neoantigens presented across multiple HLA alleles per patient. Notably, one patient in this study who had an initial MR as indicated by a reduction in ctDNA from baseline subsequently demonstrated *HLA* LOH and a concurrent rebound in ctDNA levels, suggesting outgrowth of tumor cells escaping immune pressure. A second patient, who had a monoallelic, loss-of-function mutation in *B2M*[25,26] at treatment onset also acquired *HLA* LOH over the course of vaccination, suggesting immune escape and providing a possible explanation for the observed lack of efficacy in this patient. The targeting of multiple antigens, presented by multiple HLAs in the same patient, may be an important approach to limit immune evasion and increase durable tumor control, a benefit that multiepitope vaccines would offer over adoptive T cell therapies that target only one peptide/HLA complex.

The phase 1 interim data described herein demonstrate the safety, tolerability, immunogenicity and preliminary clinical efficacy of a shared neoantigen vaccine. Analysis of vaccine-elicited T cell responses in patients provided important insights into how immune dominant neoepitopes can skew the immune response towards HLA matched epitopes that are encoded by the cassette but not presented by the tumor, weakening the potency of the vaccine. These results demonstrate that antigen presentation, target density and immunogenicity are closely linked and must be considered when designing multiepitope vaccines. This has important implications for the design of future tumor antigen vaccines, as antigens within the same vaccine cassette can compete, and therefore, selection of fewer and highly relevant tumor neoepitopes may be a better strategy than delivery of large numbers of neoepitopes without prior selection. One approach to consider may be to generate a library of single neoepitope 'off-the-shelf' vaccines that could be selected from or blended together to match the tumor mutation(s) for each patient or utilized for specific indications with high prevalence of a particular mutation. These observations have led to the generation of an optimized shared neoantigen vaccine, SLATE–KRAS, which improves upon the SLATEv1 vaccine by focusing on four highly prevalent KRAS neoantigens, each of which is repeated four times. This optimized vaccine was evaluated in a subset of patients in the phase 2 part of this study (NCT03953235), which is now completed and under analyses. Looking forward, future shared neoantigen vaccines should aim at incorporating additional classes of antigens shared between patients to increase the number of tumor and vaccine-matched antigens per patient, preferably presented by different HLAs to drive broad tumor-specific T cell responses and decrease the likelihood of immune escape. This work highlights the importance of understanding how the incorporation of multiple antigens into a vaccine may impact immunogenicity to guide vaccine design to ensure clinical candidates drive strong and broad immune responses that can offer long-term benefit to patients with cancer.

Online content

Any methods, additional references, Nature Portfolio reporting summaries, source data, extended data, supplementary information, acknowledgements, peer review information; details of author contributions and competing interests; and statements of data and code availability are available at https://doi.org/10.1038/s41591-024-02851-9.

References

1. Keenan, T. E., Burke, K. P. & Van Allen, E. M. Genomic correlates of response to immune checkpoint blockade. *Nat. Med.* **25**, 389–402 (2019).
2. Rizvi, N. A. et al. Cancer immunology. Mutational landscape determines sensitivity to PD-1 blockade in non-small cell lung cancer. *Science* **348**, 124–128 (2015).
3. Palmer, C. D. et al. Individualized, heterologous chimpanzee adenovirus and self-amplifying mRNA neoantigen vaccine for advanced metastatic solid tumors: phase 1 trial interim results. *Nat. Med.* **28**, 1619–1629 (2022).
4. Prior, I. A., Hood, F. E. & Hartley, J. L. The frequency of Ras mutations in cancer. *Cancer Res.* **80**, 2969–2974 (2020).
5. Hong, D. S. et al. *KRAS*^{G12C} inhibition with sotorasib in advanced solid tumors. *N. Engl. J. Med.* **383**, 1207–1217 (2020).
6. Jänne, P. A. et al. Adagrasib in non-small cell lung cancer harboring a *KRAS*^{G12C} mutation. *N. Engl. J. Med.* **387**, 120–131 (2022).
7. Kim, D., Xue, J. Y. & Lito, P. Targeting *KRAS*^{G12C}: from inhibitory mechanism to modulation of antitumor effects in patients. *Cell* **183**, 850–859 (2020).
8. Skoulidis, F. et al. Sotorasib for lung cancers with *KRAS*^{G12C} mutation. *N. Engl. J. Med.* **384**, 2371–2381 (2021).
9. Awad, M. M. et al. Acquired resistance to *KRAS*^{G12C} inhibition in cancer. *N. Engl. J. Med.* **384**, 2382–2393 (2021).
10. Canon, J. et al. The clinical *KRAS*^{G12C} inhibitor AMG 510 drives anti-tumour immunity. *Nature* **575**, 217–223 (2019).
11. Bulik-Sullivan, B. et al. Deep learning using tumor HLA peptide mass spectrometry datasets improves neoantigen identification. *Nat. Biotechnol.* **37**, 55–63 (2019).
12. Fourcade, J. et al. PD-1 and Tim-3 regulate the expansion of tumor antigen-specific CD8$^+$ T cells induced by melanoma vaccines. *Cancer Res.* **74**, 1045–1055 (2014).
13. Tran, E. et al. T cell transfer therapy targeting mutant *KRAS* in cancer. *N. Engl. J. Med.* **375**, 2255–2262 (2016).
14. Maiers, M., Gragert, L. & Klitz, W. High-resolution HLA alleles and haplotypes in the United States population. *Hum. Immunol.* **68**, 779–788 (2007).
15. Cerami, E. et al. The cBio cancer genomics portal: an open platform for exploring multidimensional cancer genomics data. *Cancer Discov.* **2**, 401–404 (2012).
16. de Bruijn, I. et al. Analysis and visualization of longitudinal genomic and clinical data from the AACR Project GENIE Biopharma Collaborative in cBioPortal. *Cancer Res.* **83**, 3861–3867 (2023).
17. Gao, J. et al. Integrative analysis of complex cancer genomics and clinical profiles using the cBioPortal. *Sci. Signal.* **6**, pl1 (2013).
18. Guo, W., Wang, S. J., Yang, S., Lynn, H. & Ji, Y. A Bayesian interval dose-finding design addressing Ockham's razor: mTPI-2. *Contemp. Clin. Trials* **58**, 23–33 (2017).
19. Ji, Y. & Wang, S. J. Modified toxicity probability interval design: a safer and more reliable method than the 3+3 design for practical phase I trials. *J. Clin. Oncol.* **31**, 1785–1791 (2013).
20. Ramos-Casals, M. et al. Immune-related adverse events of checkpoint inhibitors. *Nat. Rev. Dis. Prim.* **6**, 38 (2020).
21. Vega, D. M. et al. Changes in circulating tumor DNA reflect clinical benefit across multiple studies of patients with non-small-cell lung cancer treated with immune checkpoint inhibitors. *JCO Precis. Oncol.* **6**, e2100372 (2022).
22. Bratman, S. V. et al. Personalized circulating tumor DNA analysis as a predictive biomarker in solid tumor patients treated with pembrolizumab. *Nat. Cancer* **1**, 873–881 (2020).
23. Sivapalan L. et al. Liquid biopsy approaches to capture tumor evolution and clinical outcomes during cancer immunotherapy. *J. Immunother. Cancer* https://doi.org/10.1136/jitc-2022-005924 (2023).
24. Assaf, Z. J. F. et al. A longitudinal circulating tumor DNA-based model associated with survival in metastatic non-small-cell lung cancer. *Nat. Med.* **29**, 859–868 (2023).
25. Gettinger, S. et al. Impaired HLA class I antigen processing and presentation as a mechanism of acquired resistance to immune checkpoint inhibitors in lung cancer. *Cancer Discov.* **7**, 1420–1435 (2017).
26. Schoenfeld, A. J. & Hellmann, M. D. Acquired resistance to immune checkpoint inhibitors. *Cancer Cell* **37**, 443–455 (2020).
27. Rodriguez, F., Harkins, S., Slifka, M. K. & Whitton, J. L. Immunodominance in virus-induced CD8$^+$ T cell responses is dramatically modified by DNA immunization and is regulated by gamma interferon. *J. Virol.* **76**, 4251–4259 (2002).
28. Carbone, D. P. et al. Immunization with mutant p53- and K-Ras-derived peptides in cancer patients: immune response and clinical outcome. *J. Clin. Oncol.* **23**, 5099–5107 (2005).
29. Folegatti, P. M. et al. Safety and immunogenicity of the ChAdOx1 nCoV-19 vaccine against SARS-CoV-2: a preliminary report of a phase 1/2, single-blind, randomised controlled trial. *Lancet* **396**, 467–478 (2020).
30. Shaw, A. R. & Suzuki, M. Immunology of adenoviral vectors in cancer therapy. *Mol. Ther. Methods Clin. Dev.* **15**, 418–429 (2019).
31. Ogwang, C. et al. Prime-boost vaccination with chimpanzee adenovirus and modified vaccinia Ankara encoding TRAP provides partial protection against *Plasmodium falciparum* infection in Kenyan adults. *Sci. Transl. Med.* **7**, 286re5 (2015).
32. Schreiber, H., Wu, T. H., Nachman, J. & Kast, W. M. Immunodominance and tumor escape. *Semin. Cancer Biol.* **12**, 25–31 (2002).
33. Burger, M. L. et al. Antigen dominance hierarchies shape TCF1$^+$ progenitor CD8 T cell phenotypes in tumors. *Cell* **184**, 4996–5014.e26 (2021).
34. Friedman, J. et al. Neoadjuvant PD-1 immune checkpoint blockade reverses functional immunodominance among tumor antigen-specific T cells. *Clin. Cancer Res.* **26**, 679–689 (2020).

Amy R. Rappaport[1], Chrisann Kyi[2], Monica Lane[1], Meghan G. Hart[1], Melissa L. Johnson[3], Brian S. Henick[4], Chih-Yi Liao[5], Amit Mahipal[6], Ardaman Shergill[5], Alexander I. Spira[7], Jonathan W. Goldman[8], Ciaran D. Scallan[1], Desiree Schenk[1], Christine D. Palmer[1], Matthew J. Davis[1], Sonia Kounlavouth[1], Lindsey Kemp[1], Aaron Yang[1], Yaojun John Li[1], Molly Likes[1], Annie Shen[1], Gregory R. Boucher[1], Milana Egorova[1], Robert L. Veres[1], J. Aaron Espinosa[1], Jason R. Jaroslavsky[1], Lauren D. Kraemer Tardif[1], Lindsey Acrebuche[1], Christopher Puccia[1], Leiliane Sousa[1], Rita Zhou[1], Kyounghwa Bae[1], J. Randolph Hecht[8], David P. Carbone[9], Benny Johnson[10], Andrew Allen[1], Andrew R. Ferguson[1] & Karin Jooss[1] ✉

[1]Gritstone bio, Emeryville, CA, USA. [2]Memorial Sloan Kettering Cancer Center, New York, NY, USA. [3]Sarah Cannon Research Institute, Nashville, TN, USA. [4]Columbia University Herbert Irving Comprehensive Cancer Center, New York, NY, USA. [5]University of Chicago Medical Center and Biological Sciences, Chicago, IL, USA. [6]Mayo Clinic, Rochester, MN, USA. [7]Virginia Cancer Specialists, Fairfax, VA, USA. [8]University of California, Los Angeles, Los Angeles, CA, USA. [9]The Ohio State University Comprehensive Cancer Center, Columbus, OH, USA. [10]MD Anderson Cancer Center, Houston, TX, USA.
✉e-mail: kjooss@gritstone.com

Methods

Ethics statement

The research presented in this manuscript complies with all the relevant ethical regulations. Animal studies were performed according to the Institutional Animal Care and Use Committee approved protocol at Murigenics. The clinical study and all related analyses were carried out in accordance with the Declaration of Helsinki and Good Clinical Practice guidelines and were approved by the appropriate institutional review board (IRB) or ethics committees at each participating site. All patients provided written, informed consent. Further details can be found at https://clinicaltrials.gov/ct2/show/NCT03953235.

Mouse studies

Animal selection and dosing. Studies were conducted at Murigenics under the Institutional Animal Care and Use Committee approved protocols. Transgenic mice heterozygous for a transgene encoding a chimeric class I molecule consisting of human HLA were used to assess immune responses to human tumor neoantigens. The following strains were used: HLA-A11:01 (no. 9660), HLA-A2:01 (no. 9659) and HLA-A1:01 (no. 9662). All transgenic mice were obtained from Taconic and are on a CB6F1 background. C57BL6 mice (Envigo) were used as unvaccinated controls and for evaluation of mouse antigen vaccines. Female HLA-transgenic or C57BL6 mice (>6 weeks old) were immunized IM bilaterally into the anterior tibialis muscle with ChAd or samRNA (50 µl per leg). Mice were housed in ventilated cage racks with microfiltered tops and sterile bedding. They were provided with irradiated food and sterile water ad libitum. Mice were housed at 19–21 °C and 50 ± 20% relative humidity, in rooms with at least ten room air changes per hour. The photoperiod was diurnal (12 h light and 12 h dark).

Splenocyte isolation. Mouse spleens were extracted 14 days following immunization. The spleens were suspended in Roswell Park Memorial Institute (RPMI) complete (RPMI + 10% fetal bovine serum) media and dissociated using the gentle MACS Dissociator (Milltenyi Biotec). Dissociated cells were filtered using a 40 µm strainer, and then, red blood cells were lysed with ACK lysing buffer (150 mM NH_4Cl, 10 mM $KHCO_3$ and 0.1 mM ethylenediaminetetraacetic acid (EDTA)). Following lysis, cells were filtered with a 30-µm strainer and resuspended in RPMI complete.

IFNγ ELISpot analysis (mouse). IFNγ ELISpot assays were performed using precoated 96-well plates (MAbtech, Mouse IFNγ ELISpot PLUS, ALP) following manufacturer's protocol. The samples were stimulated overnight with a peptide pool containing all possible minimal epitopes (38 peptides) spanning the 25mer for each neoantigen at a final concentration of 5 µg ml^{-1} per peptide (Genscript). The response to the universal pan-DR epitope (PADRE) epitope encoded in each cassette was assessed with stimulation with the PADRE peptide (AKFVAAWTLKAAA) at 10 µg ml^{-1}. The splenocytes were plated in duplicate at 2×10^5 cells per well for KRAS Q61H, 2.5×10^4 cells per well (mixed with 7.5×10^4 naive C57B6 splenocytes) for TP53-S127Y or 1×10^5 cells per well for PADRE and all other peptide pools. A dimethyl sulfoxide (DMSO)-only control was plated for each sample and cell number. Phorbol myristate acetate and ionomycin-stimulated wells were included on each plate. Following overnight incubation at 37 °C, plates were washed with phosphate-buffered saline (PBS) and incubated with anti-mouse IFNγ mAb biotin (Mabtech) for 2 h, followed by an additional wash and incubation with Streptavidin-ALP (Mabtech) for 1 h. After final wash, plates were incubated for 10 min with BCIP/NBT (Mabtech) to develop the immune spots. Spots were imaged and enumerated using an AID reader using the vSpot 7.0 software (Autoimmun Diagnostika). For data processing and analysis, samples with a replicate well variability (variability = variance/(median + 1)) greater than ten and median greater than ten were excluded[35]. Spot values were adjusted on the basis of the well saturation according to the following formula[36]:

$$\text{AdjustedSpots} = \text{RawSpots} + 2 \times (\text{RawSpots} \times \text{Saturation}/(100 - \text{Saturation}))$$

Each sample was background corrected by subtracting the average value of the negative control peptide wells. The data are presented as SFU per 1×10^6 splenocytes. Wells with well saturation values greater than 35% were labeled as 'too numerous to count' and set to the maximum value (13,000 SFU/10^6). LOD was defined as the average value for all naive samples + standard deviation (s.d.), set to 33. The samples less than LOD were set to LOD.

Monoallelic cell lines generation and culture

The K562 HLA A*11:01 cells used for cassette format evaluation were generated using the pMSCVP vector. HLA A*11:01 retrovirus was generated using Phoenix-ampho cells transduced with lipofectamine according to manufacturer's instructions, with supernatant collection at 48 h and 72 h. K562 parental lines were transduced with the pooled virus and selected with 1 µg ml^{-1} of puromycin to generate an HLA monoallelic line. For the epitope cassettes, constructs (SLATE 20×1, KRAS 4×1, KRAS 4×1 + TP53-R213L, KRAS 4×1 + TP53-S127Y, KRAS 1×4 G12D, KRAS 1×4 G12V and KRAS 4×4) were cloned into pLxCMT vector; then the lentivirus was prepared from each construct transfected into 293T cells using a ViraPower Lentivirus Packaging mix (Thermo) and Lipofectamine 2000. The lentivirus was collected at 48 h and 72 h post-transfection, concentrated using ultracentrifuge filters (Amicon) and then titrated using Lenti-X qRT–PCR Titration Kit (TAKARA). The K562 HLA A*11:01 stable monoallelic line was transduced at 100 multiplicity of infection and selected with 20 µg ml^{-1} blasticidin. After multiple rounds of selection, stable lines were grown in IMDM, 10% fetal bovine serum, 0.5% PenStrep, 0.3 µg ml^{-1} puromycin, 20 µg ml^{-1} blasticidin (GIBCO) and expanded for HLA-A and PADRE expression evaluation and targeted MS analysis (approximately $400–500 \times 10^6$ cells). For MS validation of additional shared neoantigens in SLATEv1 in other alleles, additional monoallelic lines were generated with respective HLA constructs (HLA-A*01:01, HLA-A*02:01, HLA-A*03:01, HLA-A*68:01, HLA-B*07:02 and HLA-C*03:04) and either SLATE 20×1 or KRAS 4×4 constructs as described above. One HLA-A*02:01 K562 monoallelic line was additionally transduced with KRAS-G12C 25mer minigene construct similarly to above but at 5,000 multiplicity of infection, followed by selection under blasticidin to obtain a very high expressing line to determine KRAS-G12C HLA processing and presentation.

Tumor specimens for MS validation of epitope validation

Tumor specimens (0.5–1 g) were procured from commercial biorepository or directly from surgical centers. Colorectal carcinoma and high-grade serous ovarian carcinoma tumor specimens were sourced from Proteogenex, and a lung adenocarcinoma specimen was obtained from Marie Lannelongue Hospital Thoracic Surgery Center. All clinical materials were obtained with appropriate IRB/independent ethics committee approval.

Assessment of HLA and SLATE cassette expression levels by qPCR

Expression levels of the HLA allele and cassettes (PADRE) were determined by qPCR (Taqman). Cell lines samples were collected (1×10^6 cells per sample), washed once with PBS and lysed in RNeasy Lysis Buffer RLT (Qiagen) and 1% β-mercaptoethanol. The lysate was transferred to a 96-well KingFisher Flex, and RNA was extracted using Omega Bio-Tek's Mag-Bind Total RNA 96 Kit with a customized protocol, eluting in 50 µl of RNA Elution Buffer. RNA was quantified using Quant-iT Ribogreen RNA Assay Kit from Invitrogen. RNA quality was spot checked by running an RNA ScreenTape from Agilent. Extracted RNA (250 ng) was used

as template for cDNA synthesis using SuperScript IV VILO Master Mix with ezDNase as per manufacturer protocol. The qPCR reaction was performed in duplicate using cDNA template, 1× TaqMan Gene Expression Master Mix and 1× custom TaqMan assay Gene Expression probes (HLA A- Hs01058806_g1; PADRE (SLATE cassette)—Custom Plus TaqMan RNA Assay, FAM; TBP—Hs00427620_m1) from Life Technologies. The qPCR reaction was performed in a thermocycler and fold expression changes calculated using Ct values normalized to the TBP housekeeping gene using the equation $2^{-\Delta\Delta CT}$.

Heavy isotope-labeled HLA-peptide monomer standards

To generate the heavy isotope-labeled HLA/peptide monomers, the heavy chain and light chain (β2m) of the HLA-class I allele A*11:01 were expressed in inclusion bodies using BL21 *Escherichia coli* and a pET28a vector. The bacterial pellet was subjected to sonication in Millipore-Sigm Bugbuste Master Mix followed by washes with 50 mM Tris HCl, 100 mM NaCl, 1 mM EDTA and 0.5% Triton X-100 pH 8 and washes with 50 mM Tris HCl, 100 mM NaCl and 1 mM EDTA pH 8. Following centrifugation, to obtain the inclusion body pellet, inclusion bodies were resuspended in 8 M urea, 25 mM MES, 10 mM EDTA and 10 mM dithiothreitol. The HLA was then refolded in the presence of stable isotope-labeled peptide (single amino acid either lysine or leucine-N15/C13) to generate the HLA/peptide complex. Briefly, 10 mg of β2m was added to 100 mM Tris HCl, 400 mM L-arginine hydrochloride, 2 mM EDTA, 1.5 mM reduced glutathione and 0.5 mM oxidized glutathione. Then, 5 mg of heavy isotope-labeled peptide resuspended in DMSO was added, followed by 10 mg of heavy chain. The HLA/peptide complex was then left to refold overnight. The refolded HLA/peptide complex was concentrated and purified usingFPLC with a GE HiLoad 26/600 Superdex 200 pg column equilibrated in 20 mM Tris and 50 mM NaCl pH 8. Fractions containing the HLA/peptide complex were pooled and concentrated. Concentration of each hpHLA was determined by nanoflow liquid chromatography–mass spectrometry against known quantity of matching double labeled standard (labeled at second site either arginine, leucine or valine), which when spiked into hpHLA standard complexes and following trifluoroacetic acid addition were eluted from 10 K molecular weight cutoff filter tubes along with peptides dissociated from complexes. Cysteine-containing peptides were treated to additional dithiothreitol reduction and iodoacetamide alkylation at pH 8 before acid addition.

Targeted immunopeptomic analysis of engineered K562 cell lines

Cell pellets of 5×10^8 cells or pulverized fresh frozen tumor tissues were lysed in 20 mM Tris, 150 mM sodium chloride, 1% CA-630, pH 8 in the presence of phosphatase and protease inhibitors (Thermo) and 5 mM EDTA. Samples were rotated at 4 °C for 1 h and then spun to pellet cell debris. Cleared lysates were combined with 100–2,000 fmol of hpHLA standards, filtered through glass filter plate (Agilent) and then added to W632-pan class I-specific antibody-bound NHS-Sepharose beads atop a second filter plate (Agilent). Lysates were washed under vacuum three times each in succession with of 20 mM Tris pH 8 with 0, 150 and 500 mM NaCl. Peptides were eluted by adding 200 µl of 2 N acetic acid or 2% trifluoroacetic acid.

The eluted peptides were desalted and separated from HLA molecules desalted and separated from the HLA using a 25-mg Sep Pak (Waters) with 30% acetonitrile in 0.1% formic acid before partial dry down in evaporator (GenVac EZ-2 Plus). Peptide solutions were adjusted to pH 8 with Tris buffer and then treated with dithiothreitol followed by iodoacetamide to reduce and alkylate free cysteines. The solutions were acidified with additional trifluoroacetic acid and then desalted over a 3-mg HLB plate (Waters). Peptides eluted with 30% acetonitrile in 0.1% formic acid were then taken to dryness in evaporator, followed by resuspension in 10 µl of 3% acetonitrile and 0.1% formic acid with the appropriate heavy isotope standards. Resuspended samples were analyzed by targeted MS using an EASY-nLC coupled to an Orbitrap Fusion Lumos Tribrid mass spectrometer with a nano-electrospray ion source. The EASY-nLC was set up with a 75 µm × 2 cm PepMap 100 precolumn (Thermo) followed by a 75 µm × 25 cm PepMap 100 C18 analytical column (Thermo). A 180-min linear gradient starting with 4% acetonitrile and 0.1% formic acid and ending at 40% acetonitrile and 0.1% formic acid was used to elute the sample. Data were acquired in parallel reaction monitoring (PRM) targeted MS mode with an isolation window of 0.7 *m/z*, fixed collision energy of 28 and at a resolution of 30,000. An automatic gain control target of 5×10^4 and maximum injection time of 54 ms was used for each MS2 scan. A full MS scan was also acquired every cycle with a resolution of 60,000, automatic gain control target of 4×10^5, maximum injection time of 50 ms and scan range of 300–2,000 *m/z*. The target lists containing the precursor masses to be isolated and fragmented for each sample injection were created from a list of KRAS, TP53 and additional SLATE neoantigen peptides. Data were processed using Skyline (University of Washington, MacCoss Lab). Spectral peak list outputs were imported into the ProteomicsDB Universal Spectrum Explorer[37] for butterfly visualizations.

Phase 1 clinical trial

Study design. The study protocol is available in Supplementary Information. This phase 1 study is part of a phase 1/2 study designed to assess the safety and tolerability, RP2D, early clinical activity and immunogenicity of GRT-C903 (ChAd68) and GRT-R904 (samRNA), a neoantigen-based therapeutic cancer vaccine in combination with ICB in patients with metastatic solid tumors. Once an RP2D was identified in phase 1, tumor-specific expansion cohorts and a cohort of mutation-positive tumors outside of treatment settings in tumor types already represented by other expansion cohorts were explored in phase 2.

The first patient enrolled on 18 July 2019, and the last patient enrolled on 12 March 2020 for the phase 1 portion of the study. As of the data cutoff date of 4 March 2023, a total of 39 patients, that is, 19 patients in phase 1 and 20 patients in phase 2, had been treated. The study is still ongoing to evaluate the efficacy of the RP2D using ORR, duration of response, CBR, PFS and OS. There were four protocol amendments, but none of these amendments occurred during the phase 1 enrollment period, and the protocol changes did not impact alter treatment or assessments of patients in the phase 1 portion of the study. Ten clinical sites enrolled patients in phase 1, including the University of California Los Angeles, the University of Chicago Comprehensive Cancer Center, City of Hope, Columbia University Medical Center, Mayo Clinic Rochester, Mayo Clinic Jacksonville, MD Anderson Cancer Center, Memorial Sloan Kettering Cancer Center, Sarah Cannon Research Institute and Virginia Cancer Specialists. There is no data safety monitoring board for this study. A study committee consisting of the investigators and study sponsor met regularly to assess the safety profile of the study treatment and make recommendations for dose escalation. Patient data were collected via electronic data capture and analyzed as described in the statistics section.

This study was carried out in accordance with the Declaration of Helsinki and Good Clinical Practice guidelines and was approved by the appropriate IRB or ethics committees at each participating site.

Study population

Inclusion criteria for the HLA screening stage. Patients must meet the following criteria to be eligible for HLA screening:

1. Provide a signed and dated informed consent form document before collection of blood for HLA typing.
2. Patients with advanced or metastatic:
    a. Microsatellite stable (MSS)-CRC who are currently receiving systemic treatment with a fluoropyrimidine and oxaliplatin and/or irinotecan that may include a vascular endothelial

growth factor (VEGF)- or epidermal growth factor receptor (EGFR)-targeting therapy as their 1 liter or 2 liter therapy for metastatic disease or who have experienced disease progression following treatment with a fluoropyrimidine, oxaliplatin and irinotecan that may include a VEGF- or EGFR-targeting therapy but have not initiated a new line of therapy.

b. NSCLC who are currently receiving systemic treatment with an anti-PD-(L)1 antibody in combination with cytotoxic, platinum-based chemotherapy or who have experienced disease progression following treatment an anti-PD-(L)1 antibody in combination with cytotoxic, platinum-based chemotherapy (or anti-PD-(L)1 alone if patient refuses platinum-based chemotherapy) but have not initiated a new line of therapy.

c. PDA who are currently receiving systemic cytotoxic chemotherapy as their 1 liter therapy for metastatic disease or who have experienced disease progression on 1 liter systemic cytotoxic chemotherapy but have not initiated a new line of therapy.

d. Any solid tumor histology where the patient has experienced disease progression with all available therapies known to confer clinical benefit.

3. Patient's tumor possesses one of the mutations listed in the protocol table as determined per local institutional standard.
4. Patients must be greater than or equal to 18 years of age.

Exclusion criteria for the HLA screening stage. Patients meeting any of the following criteria are not eligible for HLA screening:

1. Tumors with genetic characteristics as follows:
   a. For NSCLC, patients with a known genetic driver alteration in *EGFR*, *ALK*, *ROS1*, *RET* or TRK.
   b. Patients with known microsatellite instability high (MSI^{hi}) disease based on institutional standard.
2. Known exposure to chimpanzee adenovirus or any history of anaphylaxis in reaction to a vaccination or hypersensitivity to study drug components.
3. Bleeding disorder (for example, factor deficiency or coagulopathy) or history of significant bruising or bleeding following IM injections or blood draws. If being treated with anticoagulopathy therapy, the patient must be able to withhold treatment before and after vaccination to prevent any potential bleeding complications.

Study treatment stage

Inclusion criteria for study treatment stage. Patients must meet the following inclusion criteria to be eligible for study treatment:

1. If the patient did not participate in the HLA screening stage, the patient has been enrolled in the screening protocol GO-003.
2. Provide a signed and dated informed consent form document before initiation of study-specific procedures.
3. Patients with advanced or metastatic:

   i. For phase 1, patients with:
      a. MSS-CRC who have received at least 16 weeks of 1 liter or 2 liter therapy including a fluoropyrimidine and oxaliplatin and/or irinotecan that may include a VEGF- or EGFR-targeting therapy and have not experienced disease progression or have progressed on/after therapy including fluoropyrimidine, oxaliplatin and irinotecan that may include a VEGF- or EGFR-targeting therapy.
      b. NSCLC who have experienced disease progression following treatment an anti-PD-(L)1 antibody in combination with cytotoxic, platinum-based chemotherapy (or anti-PD-(L)1 alone if the patient refuses platinum-based chemotherapy).
      c. PDA who have received at least 16 weeks of 1 liter systemic, cytotoxic chemotherapy and have not experienced disease progression or have progressed on/after first-line systemic treatment with cytotoxic chemotherapy.
      d. Patients with a solid tumor not represented in 3ia–3ic that is positive for at least one of the 20 neoantigens contained in GRT-C903/GRT-R904 and has experienced disease progression with all available therapies known to confer clinical benefit.

   i. For phase 2, patients with:
      a. Cohort 1 (MSS-CRC 1 liter or 2 liter maintenance): MSS-CRC after receiving at least 16 weeks of 1 liter or 2 liter therapy including a fluoropyrimidine and oxaliplatin and/or irinotecan that may include a VEGF- or EGFR-targeting therapy and have not experienced disease progression.
      b. Cohort 2 (MSS-CRC 3 liter): MSS-CRC who have progressed on/after therapy including fluoropyrimidine, oxaliplatin and irinotecan that may include a VEGF- or EGFR-targeting therapy.
      c. Cohort 3 (NSCLC 2 liter): NSCLC who have experienced disease progression following treatment an anti-PD-(L)1 antibody in combination with cytotoxic, platinum-based chemotherapy (or anti-PD-(L)1 alone if patient refuses platinum-based chemotherapy).
      d. Cohort 4 (PDA 1 liter maintenance): PDA who have received at least 16 weeks of 1 liter systemic, cytotoxic chemotherapy and have not experienced disease progression.
      e. Cohort 5 (PDA 2 liter): PDA who have progressed on/after 1 liter systemic treatment with cytotoxic chemotherapy.
      f. Cohort 6 (solid tumor): patients with a tumor histology not included in cohorts 1–5 that is positive for at least one of the 20 neoantigens contained in GRT-C903/GRT-R904 and has experienced disease progression following treatment with all available therapies known to confer clinical benefit.

4. Measurable disease according to RECIST v1.1.
5. Life expectancy of >3 months per the investigator.
6. ECOG performance status of 0 or 1.
7. Patient has adequate organ function as defined below. The sponsor may consider patients eligible despite having a laboratory value that does not meet inclusion criteria provided. The investigator reports if the patient is otherwise in good health, and the history and kinetics of the change in the laboratory value does not raise a significant safety concern over including the patient in the study nor compromise the integrity of the study data. The sponsor and investigator must agree to include any patients with a laboratory value below the defined criteria below.

   a. Peripheral white blood cell ≥2,000 mm^{-3}
   b. Absolute lymphocyte count ≥500 mm^{-3}
   c. Absolute neutrophil count ≥1,500 mm^{-3}
   d. Platelets ≥75,000 mm^{-3}
   e. Hemoglobin ≥9 g dl^{-1}
   f. Albumin ≥3.3 g dl^{-1}
   g. Serum creatinine ≤1.5× upper limit of normal (ULN) or calculated creatinine clearance >40 ml min^{-1} using the Cockcroft–Gault equation
   h. Alanine aminotransferase and aspartate aminotransferase ≤3× ULN
   i. Total serum bilirubin ≤1.5× ULN or direct bilirubin ≤1× ULN (patients with Gilbert's disease may be included if their total bilirubin is ≤3.0 mg dl^{-1})
   j. International normalized ratio or prothrombin time or partial thromboplastin time ≤1.5× ULN, unless the patient is receiving

anticoagulant therapy, in which case patients are eligible if prothrombin time and partial thromboplastin time are within therapeutic range of intended use of anticoagulants.
8. Patient agrees to undergo research biopsies before study treatment and approximately 8–12 weeks after the first vaccine administration if lesions are amenable to biopsy.
9. If woman of childbearing potential, willing to undergo pregnancy testing and agrees to use at least one highly effective contraceptive method during the study treatment period and for 5 months after last investigational study treatment.
10. If male and sexually active with a woman of childbearing potential, must agree to use highly effective contraception such as latex condom plus partner use of a highly effective contraceptive method during the study treatment period and for 7 months after last investigational study treatment.

Exclusion criteria for study treatment stage. Patients meeting any of the following criteria are not eligible:

1. Patient has received prior therapy consisting of anti-CTLA-4, anti-PD-1, anti-PD-L1 or any other antibody or drug specifically targeting T cell costimulation or checkpoint pathways, with the exception of patients with NSCLC or a mutation-positive solid tumor.
2. Immunosuppression from:
   - Concurrent, recent (≤4 weeks) or anticipated treatment with systemic corticosteroids (>10 mg daily prednisone equivalent) or other immunosuppressive medications such as OKT3, ATG/ALG, methotrexate, tacrolimus, cyclosporine, azathioprine or rapamycin. Inhaled or topical steroids, physiologic corticosteroid replacement therapy for adrenal or pituitary insufficiency, steroid pretreatment for chemotherapy, antihistamines, nonsteroidal anti-inflammatory drugs and aspirin are permitted in the absence of active autoimmune disease.
   - Conditions such as common variable hypogammaglobulinemia or radiation exposure such as large field radiotherapy.
3. History of allogeneic tissue/solid organ transplant.
4. Patients who have had a history of life-threatening TRAEs with prior immunotherapy or not recovered from prior cancer therapy-induced adverse events (AEs; that is, any AE that remains ≥ grade 2 or that has not returned to baseline with the exception of peripheral neuropathy, alopecia and hypothyroidism that is controlled with hormone replacement therapy or if explicitly allowed by other inclusion criteria).
5. Active, known, or suspected autoimmune disease.
   Note: patients with type I diabetes mellitus, hypothyroidism (if requiring hormone replacement), skin disorders (such as vitiligo, psoriasis or alopecia) not requiring systemic treatment or conditions not expected to recur in the absence of an external trigger are permitted. Replacement therapy (for example, thyroxine, insulin or physiologic corticosteroid replacement therapy for adrenal or pituitary insufficiency, etc.) is not considered a form of systemic treatment.
6. History of other cancer within 2 years, with the exception of basal or squamous cell carcinoma of the skin, superficial bladder cancer or carcinoma in situ of the breast, cervix, prostate or other neoplasm that has undergone potentially curative therapy with no evidence of disease recurrence.
7. Any severe concurrent noncancer disease (including active systemic infection and/or uncontrolled hypertension) that, in the judgment of the investigator, would make the patient inappropriate for the current study.
8. Active tuberculosis, recent (less than 2 weeks) clinically significant infection or evidence of active hepatitis B or hepatitis C.
9. Known history of positive test for human immunodeficiency or known acquired immunodeficiency syndrome.
10. History of pneumonitis requiring systemic steroids for treatment (with the exception of prior resolved in-field radiation pneumonitis).
11. Patient with known central nervous system metastases unless lesions have been treated by surgery and/or targeted radiotherapy and lesions have been clinically stable for at least 4 weeks. Patients with carcinomatous meningitis or treated with whole brain radiation are not eligible.
12. Myocardial infarction within 6 months of study initiation, active cardiac ischemia, myocarditis or New York Heart Association (NYHA) grade III or IV heart failure.
13. Pregnant, planning to become pregnant or nursing.
14. Received radiation therapy within 2 weeks before first dose of study treatment.
15. Treatment with botanical preparations (for example, herbal supplements or traditional Chinese medicines) intended to treat the disease under study or that may interfere with study treatment within 2 weeks before treatment.
16. Medical, psychiatric, cognitive or other conditions that compromise the patient's ability to understand the patient information, to give informed consent, to comply with the study protocol or to complete the study.

Vaccine design and manufacturing

Vaccine cassette design and manufacturing were performed as previously described[3]. Briefly, neoantigen epitopes were designed with flanking sequences so that each is 25 amino acids in length and arranged as a cassette to minimize generation of novel junction epitopes. A class II helper domain consisting of universal class II epitopes PADRE and tetanus toxoid were included at the carboxy terminus of the cassette. The cassettes were codon optimized for maximum protein expression in humans and for ease of synthesis. The cassettes were synthesized from overlapping oligonucleotides (IDT), that cover both DNA strands of the cassette sequence plus sequences in the plasmid backbones and assembled into either ChAd68 or samRNA plasmid backbones by Gibson assembly (Codex DNA). The assembled plasmids were then transformed into bacteria and screened by Sanger sequencing for correct clones, which served as the templates for GMP ChAd68 production or for samRNA transcription. ChAd68 plasmids were linearized with PacI and then transfected with TransIt Lenti (Mirus Bio) into 293F (ThermoFisher) cells to initiate virus production. The virus was amplified through successive rounds of infection before the final production run at scale. The virus was collected at 48–72 h postinfection, purified by anion exchange chromatography (Satorius GmbH) and formulated in 5 mM Tris pH 7.9, 1 mM $MgCl_2$ and 75 mM NaCl. The VP titers were determined by an absorbance at 260 nm post SDS disruption and infectious unit titers were determined by immunostaining with an anti-Ad antibody (Abcam). The samRNA plasmid was used as a template for RNA transcription using T7 polymerase, and the RNA was capped using a vaccine capping enzyme and mRNA cap 2′-*O*-methyltransferase (NEB). The RNA concentration was measured by Ribogreen quantitation and then formulated into lipid nanoparticles (Genevant).

Patient PBMC isolation and storage

Patient demographics and dosing levels are shown in Extended Data Table 2. Due to coronavirus disease 2019 restrictions, several blood draws were missed. Both ad hoc dosing and blood draw time points were added with IRB approval for several patients. Whole blood for immunogenicity testing was collected before administration of the first dose (ChAd68 prime) to assess baseline levels, and at 14 and 28 days (2 and 4 weeks) post-ChAd68 prime. Subsequent planned sample collection post samRNA boosts include days 7, 14 and 28 after dose 2 (samRNA boost no. 1) and at days 7 and/or 28 after each additional

samRNA boost. PBMCs from whole blood were isolated at local PBMC processing sites according to standardized protocols. Briefly, cells were isolated using density gradient centrifugation on Ficoll Paque Plus (GE Healthcare), washed with D-PBS (Corning), counted and cryopreserved in CryoStor CS10 (STEMCELL Technologies) at 5×10^6 cells ml^{-1}. The cryopreserved cells were stored in liquid N_2, shipped in Cryoports and transferred to storage in liquid N_2 upon arrival. The cryopreserved cells were thawed and washed twice in OpTmizer T Cell Expansion Basal Medium (Gibco) with Benzonase (EMD Millipore) and once without benzonase. The cell counts and viability were assessed using the Guava ViaCount reagents and module on the Guava EasyCyte HT cytometer (EMD Millipore). The cells were rested overnight before use in functional assays.

Peptides (clinical study)

Custom-made, recombinant, lyophilized peptides specific for each mutation were produced by Genscript (Piscataway) and reconstituted at 5 mg ml^{-1} per peptide in sterile DMSO (VWR International), aliquoted and stored at −20 °C. For each mutation, pools were made containing all possible 8–10 amino acid peptides (38 total) within the vaccine-encoded 25 amino acid length sequence. As the presentation of individual peptides by specific major histocompatibility complex class I HLA alleles had been validated by MS, and due to limited sample availability, only short peptides were assessed. Control peptides to assess responses to infectious disease antigens from CMV, EBV and Influenza (CEF peptide pool) were purchased from JPT Peptide Technologies.

IVS cultures

Neoantigen-reactive T cells from patient samples were expanded in the presence of cognate peptides and low-dose IL-2 as described previously[11]. Briefly, thawed PBMCs were rested overnight and stimulated in the presence of minimal epitope peptide pools (10 μg ml^{-1} per peptide, 38 mutation-specific minimal peptides (8–10 amino acids) per pool) or control peptides (CEF) in ImmunoCul-XF T Cell Expansion medium (IC media; STEMCELL Technologies) with 10 IU ml^{-1} rhIL-2 (R&D Systems) for 14 days in 48- or 24-well tissue culture plates. Cells were seeded at $1–2 \times 10^6$ cells per well and fed every 2–3 days by replacing two-thirds of the culture media with rhIL-2.

IFNγ ELISpot assay (clinical study)

Detection of IFNγ-producing T cells was performed by ex vivo ELISpot assay[3]. Briefly, cells were collected, counted and resuspended in media at 4×10^6 cells ml^{-1} (ex vivo PBMCs) or 2×10^6 cells ml^{-1} (IVS-expanded cells) and cultured in the presence of DMSO (VWR International) only, phytohemagglutinin-L (Sigma-Aldrich), CEF peptide pool, or cognate peptides in ELISpot Multiscreen plates (EMD Millipore) coated with anti-human IFNγ capture antibody (Mabtech). DMSO only (vehicle) wells were used as negative control and phytohemagglutinin-L stimulated wells were positive control for each sample. Control values are included in source data. Mutation-specific peptide pools containing all possible 38 minimal epitopes (8–10 amino acids) within the vaccine-encoded 25 amino acid sequence were used for stimulation at a final concentration of 10 μg ml^{-1} $peptide^{-1}$. Following 18–24 h incubation in a 5% CO_2, 37 °C, humidified incubator, supernatants were collected, cells were removed from the plate and membrane-bound IFNγ was detected using anti-human IFNγ detection antibody (Mabtech), Vectastain Avidin peroxidase complex (Vector Labs) and AEC Substrate (BD Biosciences). ELISpot plates were allowed to dry, stored protected from light and sent to Zellnet Consulting (Fort Lee) for standardized evaluation[2]. Data are presented as SFU per million cells. Positive responses were defined as mean SFU for peptide stimulated wells >LOD for all samples with mean SFU of negative control (DMSO) <LOD or mean SFU for peptide stimulated wells >2× the mean SFU of DMSO wells for samples with DMSO >LOD. Samples with DMSO values >720 SFU per million cells were excluded.

Cell-free DNA collection and isolation

Whole blood was collected in two 10-ml cell-free DNA (cfDNA) blood collection tubes (Streck) starting at the time of the prime, and subsequent draws were collected at dosing visits. Due to coronavirus disease 2019 restrictions, several blood draws were missed. Whole blood underwent a double-spin protocol to first separate plasma from white blood cells and red blood cells before a second spin to remove any remaining cellular debris. The separated plasma was frozen and shipped to Gritstone Bio and stored at −80 °C until extraction. cfDNA was extracted from the entire plasma volume of a single draw using the Apostle MiniMax cfDNA Isolation kit (ApostleBio) and quantified using the Qubit 1× dsDNA High Sensitivity Assay (Thermo Fisher Scientific).

ctDNA sequencing and analysis

A universal set of hybrid capture probes were designed to capture mutations targeted by the SLATE cassette, oncogenic hot spots and single nucleotide polymorphisms for fingerprinting. The entire coding regions of *TP53*, *PTEN*, *ARID1A* and genes involved in the antigen presentation machinery (*B2M*, *TAP1/TAP2* and *HLA-A*, *HLA-B* and *HLA-C*) were also designed for capture in the panel. The probes were designed and synthesized by Integrated DNA Technologies (IDT). Patient-matched genomic DNA from whole blood or PMBCs was fragmented before library preparation using the NEB FS module (NEB). Shotgun libraries for cfDNA (up to 30 ng) and the fragmented, patient-matched genomic DNA (20–30 ng) were prepared using the KAPA HyperPrep (KAPA Biosystems) kit using a customized pool of duplex adapters containing unique molecular identifiers (UMI) for duplex sequencing (IDT). Shotgun libraries were captured overnight using the IDT xGen Hybridization and Wash kit. Enriched libraries were sequenced on an Illumina NovaSeq to a minimum mean raw depth of 80,000×. Briefly, UMIs were clipped from the raw sequencing reads before alignment to hg38 using BWA-MEM. Using fgbio, aligned reads were grouped by position and duplex identity. Consensus reads were created using a duplex of 3× (three supporting reads from each strand) and realigned to hg38. Variant calling was performed using FreeBayes and VarDictJava[38]. The percent change in ctDNA was calculated as the change of the variant allele frequency (VAF) of the SLATE variant for enrollment from the baseline sample.

HLA analysis was performed by first extracting reads aligning to the class I *HLA* region on chr6, the *TAP1* and *TAP2* regions and unaligned reads after initial mapping to hg38. The reads were realigned to a patient-specific reference determined by enrollment genotyping for *HLA-A*, *HLA-B* and *HLA-C* using BWA-MEM. *TAP1* and *TAP2* were added to evaluate variants and private single nucleotide polymorphisms. The original duplex UMI information was transferred to the realigned reads using Genome Analysis Toolkit (GATK), and fgbio was used to group and create consensus reads from the duplex UMI and patient-specific alignment information. Consensus reads were mapped back to the patient-specific reference. HLA allele balance was calculated using the read count attributed to each patient allele as calculated by Picard. Each allele ratio was compared to the allele ratios in the patient's gDNA using a chi-square test for each *HLA* gene (A, B and C), and P values <0.05 were considered significant for *HLA* LOH.

Statistics and reproducibility

For the clinical study, the sample size was not driven by a statistical power due to the nature of an adaptive dose escalation method. The phase 1 sample size ranged from 11 to 24 patients based on the adaptive mTPI-2 design. No data were excluded from the analyses, and experiments were not randomized. The investigators were not blinded to allocation during experiments and outcome assessment. The all-treated analysis population, defined as all patients who receive any amount of study treatment, was used in the analysis, and ctDNA evaluable analysis population, defined as all patients who received any

amount of the study treatment and who have evaluable baseline ctDNA assessment and at least one postbaseline ctDNA assessment, was used for the ctDNA data analysis. The ORR was based on RECIST v. 1.1. The BOR is defined as the best response recorded from the study treatment start until disease progression or death, whichever comes earlier. PFS is defined as the date of first dose with GRT-C903 to the earliest date of progression or death by any cause (in the absence of progression). OS is measured from the date of the first dose of GRT-C903 to the date of death by any cause. OS time for patients alive by the end of the study will be censored at the last date that the patient surviving status is known. The median PFS and OS were estimated by the Kaplan–Meier method, and the corresponding two-sided 95% confidence intervals were calculated according to the Brookmeyer and Crowley method. Analysis was performed using SAS 9.4. AEs were coded using the Medical Dictionary for Regulatory Activities v 21.1. Common terminology criteria for AEs were used to grade the severity of AEs. A treatment-emergent AE is defined as any AE with onset after the administration of study medication through 100 days post-treatment or initiation of alternative anticancer therapy, whichever occurred first, or any event that was present at baseline but worsened in intensity or was subsequently considered drug-related by the investigator through the end of the study.

Reporting summary

Further information on research design is available in the Nature Portfolio Reporting Summary linked to this article.

Data availability

Deidentified individual participant clinical data that underlie the results reported in this article are available for transfer. Interested investigators can obtain and certify the data transfer agreement and submit requests to the principal investigator K.J. Investigators and institutions who consent to the terms of the data transfer agreement form, including, but not limited to, the use of these data for the purpose of a specific project and only for research purposes and to protect the confidentiality of the data and limit the possibility of identification of participants in any way whatsoever for the duration of the agreement, will be granted access. Gritstone will then facilitate the transfer of the requested deidentified data within 60 days. This mechanism is expected to be via a Gritstone Secure File Transfer Service, but Gritstone reserves the right to change the specific transfer method at any time, provided appropriate levels of access authorization and control can be maintained. Epitope selection utilized a previously published model[11]. Source data are provided with this paper.

References

35. Moodie, Z. et al. Response definition criteria for ELISPOT assays revisited. *Cancer Immunol. Immunother.* **59**, 1489–1501 (2010).
36. Janetzki, S. et al. Guidelines for the automated evaluation of Elispot assays. *Nat. Protoc.* **10**, 1098–1115 (2015).
37. USE (Universal Spectrum Explorer). *ProteomicsDB* https://www.proteomicsdb.org/use/ (2021).
38. Lai, Z. et al. VarDict: a novel and versatile variant caller for next-generation sequencing in cancer research. *Nucleic Acids Res.* **44**, e108 (2016).

Acknowledgements

The study sponsor was Gritstone bio, Inc. We thank the patients and their families; clinical staff and study coordinators; Bristol Myers Squibb for providing ipilimumab and nivolumab; and M. Marrali, K. Taquechel, J. Busby, R. Yelensky and M. Skoberne. Funding was provided by the study sponsor, Gritstone bio. Employees of Gritstone bio received salaries for study conceptualization, design, data analyses and manuscript preparation. No other authors received specific funding for this work from the sponsor.

Author contributions

A.R.R., M.L., A.R.F., M.G.H., D.S. and K.J. wrote the manuscript. A.R.R., C.D.P., M.J.D., A.R.F., M.L., A.A. and K.J. contributed to study design. A.R.R., M.L., M.G.H., D.S., C.D.P., M.J.D., L.S., L.K., S.K., G.R.B., M.E., Y.J.L., M.L., L.A., J.R.J., L.D.K.T., C.P., L.S., R.Z., A. Shen, A.Y. and K.B. contributed to experimental design, execution and data analysis. A.R.F., C.K., A.I.S., C.-Y.L., A. Shergill, M.L.J., B.S.H., D.P.C., B.J., A.M., J.R.H. and J.W.G. contributed to clinical oversight, patient recruitment, enrollment and treatment. C.D.S., R.L.V. and J.A.E. contributed to vaccine design and production.

Competing interests

A.R.R., M.L., M.G.H., C.D.S., D.S., C.D.P., M.J.D., S.K., L.K., A.Y., Y.J.L., M.L., A. Shen, G.R.B., M.E., R.L.V., J.A.E., J.R.J., L.D.K.T., L.A., C.P., L.S., R.Z., K.B., A.A., A.R.F. and K.J. are stockholders and either current or previous employees at Gritstone bio, Inc. and may be listed as co-inventors on various pending patent applications related to the vaccine platform presented in this study. C.K. received honoraria from OncLive, Total Health, consults/has consulted for Scenic Immunology BV and has received research funding from Bristol Myers Squibb, Merus, Gritstone bio and Acrivon. C.-Y.L. consults/has consulted for AstraZeneca, Genentech, Histosonics, Incyte, Ipsen, QED, Transthera and Boston Scientific and is a speaker for AstraZeneca and Incyte. A.I.S. has a leadership role at NEXT Oncology Virginia; is a stockholder of Eli Lilly; has received honoraria from CytomX Therapeutics, AstraZeneca/MedImmune, Merck, Takeda, Amgen, Janssen Oncology, Novartis, Bristol Myers Squibb and Bayer; has consultant or advisory roles at Incyte, Amgen, Novartis, Mirati Therapeutics, Gritstone bio, Jazz Pharmaceuticals, Takeda, Janssen Research & Development, Mersana, Daiichi Sankyo/AstraZeneca, Regeneron, Lilly, Black Diamond Therapeutics, Sanofi, Array BioPharma, AstraZeneca/MedImmune, Bristol Myers Squibb and Blueprint Medicines; has received research funding from LAM Therapeutics, Regeneron, Roche, AstraZeneca, Boehringer Ingelheim, Astellas Pharma, MedImmune, Novartis, Incyte, Abbvie, Ignyta, Takeda, Macrogenics, CytomX Therapeutics, Astex Pharmaceuticals, Bristol Myers Squibb, Loxo, Arch Therapeutics, Gristone bio, Plexxikon, Amgen, Daiichi Sankyo, ADCT, Janssen Oncology, Mirati Therapeutics, Rubius, Mersana, Blueprint Medicines, Alkermes, Revolution Medicines, Medikine, Synthekine, Black Diamond Therapeutics, BluPrint Oncology, Nalo Therapeutics, Scorpion Therapeutics and ArriVent Biopharma. M.L.J.: financial interests, personal, advisory board: Astellas, Otsuka; financial interests, institutional, research grant: AbbVie, Acerta, Amgen, Apexigen, Arcus, Array, AstraZeneca, Atreca, Beigene, Birdie, Boehringer Ingelheim, Checkpoint Therapeutics, Guardant Health, Genocea, Hengrui, Immunocore, Incyte, Janseen, Jounce, Gritstone bio, Lycera, Merck, Mirati, Oncomed, Regeneron, Ribon, Sanofi, Shattuck Labs, Stem CentRx, Syndax, Takeda, Tarveda, TCR2 Therapeutics, University of Michigan and WindMIL. B.J.: financial interests, personal, advisory board: Gritstone bio, Inc., Incyte, Taiho Oncology; financial interests, personal, research grant: BMS, Syntrix. A.M.: financial interests, personal, advisory board: Taiho, Incyte. J.R.H.: financial interests, personal, advisory board: Ipsen, Merck and Acrotech Biopharma; financial interests, institutional, research grant: ARMO Biosciences, Halozyme, Amgen, Merck, AbbVie, Advaxis, Astellas, Forty Seven, Immunomedics, Lilly, Gritstone bio, GSK and Arcus. The other authors declare no competing interests.

Additional information

Extended data is available for this paper at https://doi.org/10.1038/s41591-024-02851-9.

Supplementary information The online version contains supplementary material available at https://doi.org/10.1038/s41591-024-02851-9.

Correspondence and requests for materials should be addressed to Karin Jooss.

Peer review information *Nature Medicine* thanks Neeha Zaidi and the other, anonymous, reviewer(s) for their contribution to the peer review of this work. Primary Handling Editor: Saheli Sadanand, in collaboration with the *Nature Medicine* team.

https://doi.org/10.1038/s41591-024-02851-9

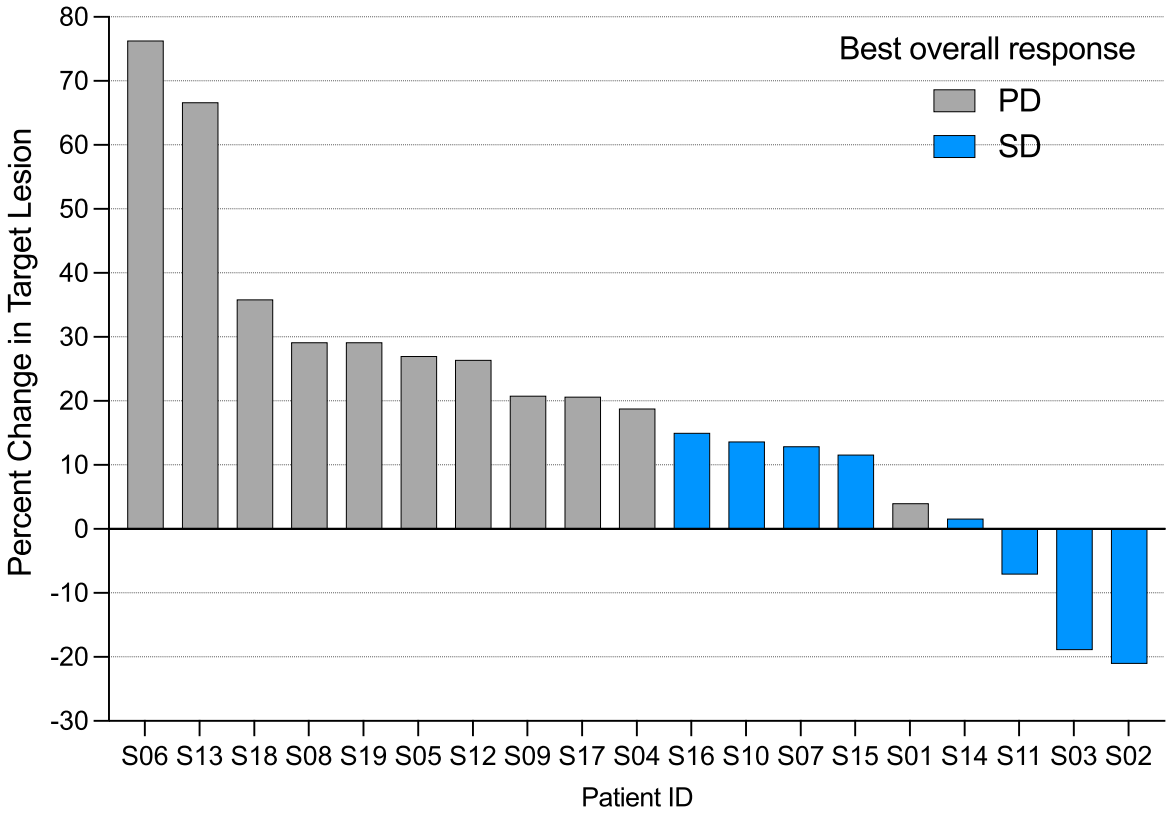

Extended Data Fig. 1 | Tumor response waterfall plot. Best percent change from baseline in target lesion for each patient ($n = 19$).

https://doi.org/10.1038/s41591-024-02851-9

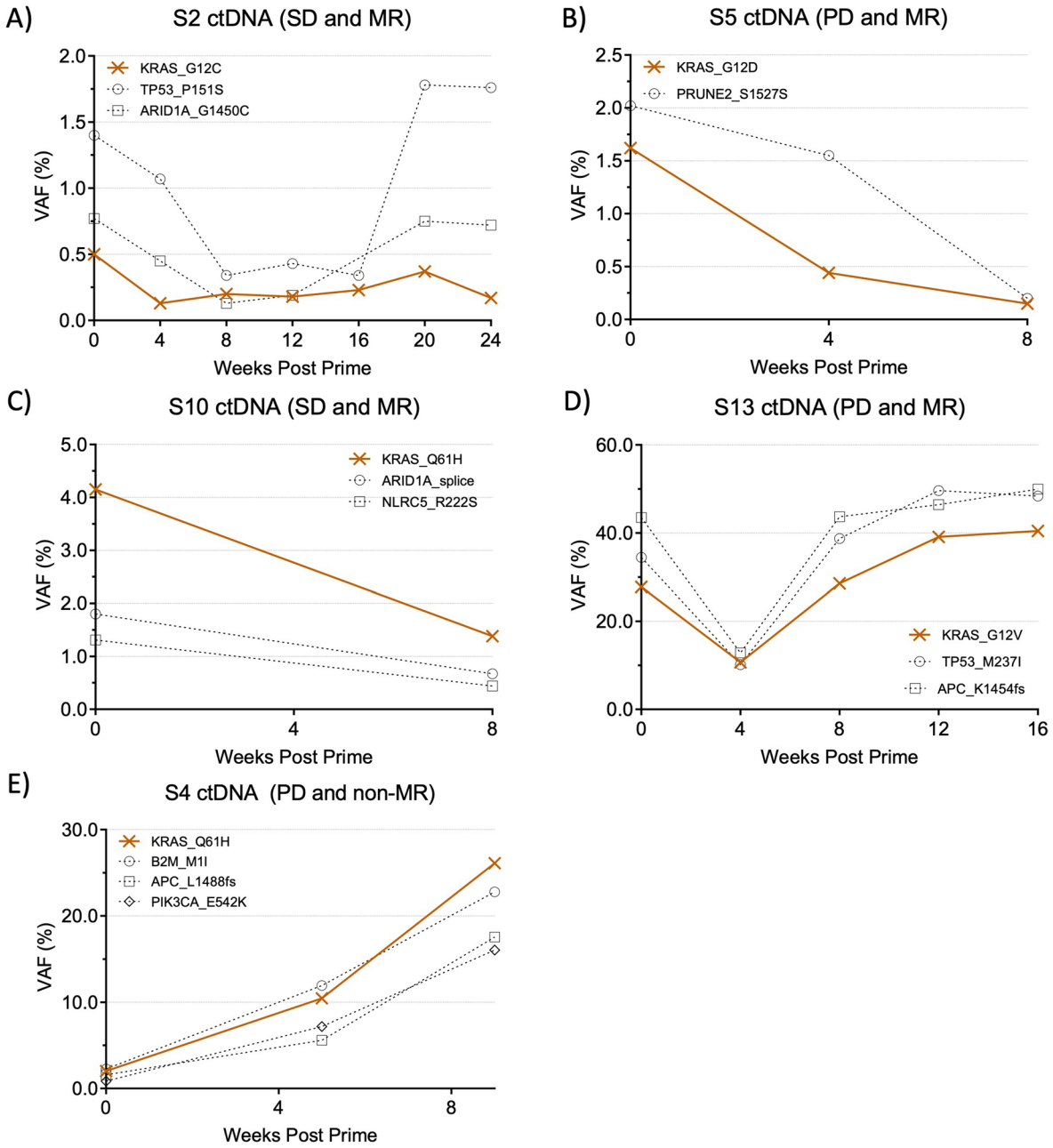

Extended Data Fig. 2 | ctDNA monitoring of tumor variants in SLATE patients. (A-E) Levels of ctDNA over time post prime vaccination for each patient for the vaccine encoded tumor mutation (orange) as well as additionally detected somatic mutations (gray). ctDNA levels reported as variant allele frequency (VAF) as a percentage of total reads. (A-D) All 4 patients with molecular response (MR) (out of 12 patients assessed), defined as > 30% decrease in vaccine encoded tumor variant compared to baseline. (E) Representative patient with no MR, showing loss of *B2M* start codon. The best overall response is denoted.

https://doi.org/10.1038/s41591-024-02851-9

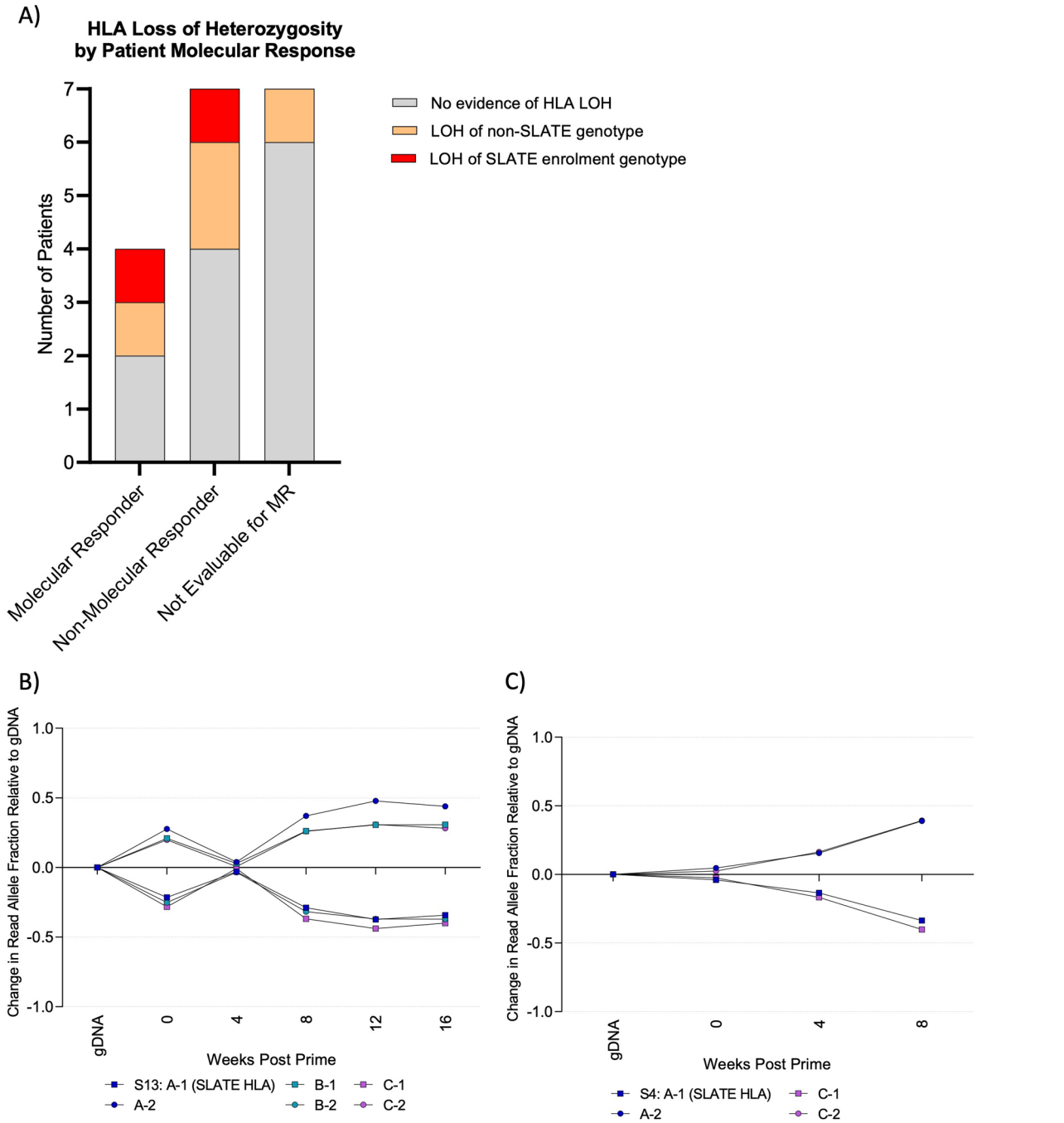

Extended Data Fig. 3 | HLA Loss of Heterozygosity. (A) *HLA* LOH was assessed in cfDNA and biopsies as described in the methods. Patient was considered LOH if LOH was detected in a biopsy or at any cfDNA timepoint. $n = 18$. Patient S1 was not assessed for *HLA* LOH due to lack of sufficient cfDNA material. (B) Longitudinal change of read allele fraction in cfDNA relative to genomic DNA (gDNA) across *HLA* class I alleles of S13, a molecular responder who demonstrated focal LOH that included the SLATE-relevant *HLA* genotype. (C) Longitudinal change of read allele fraction in cfDNA relative to gDNA of molecular non-responder S4. Patient is homozygous in *HLA-B*.

https://doi.org/10.1038/s41591-024-02851-9

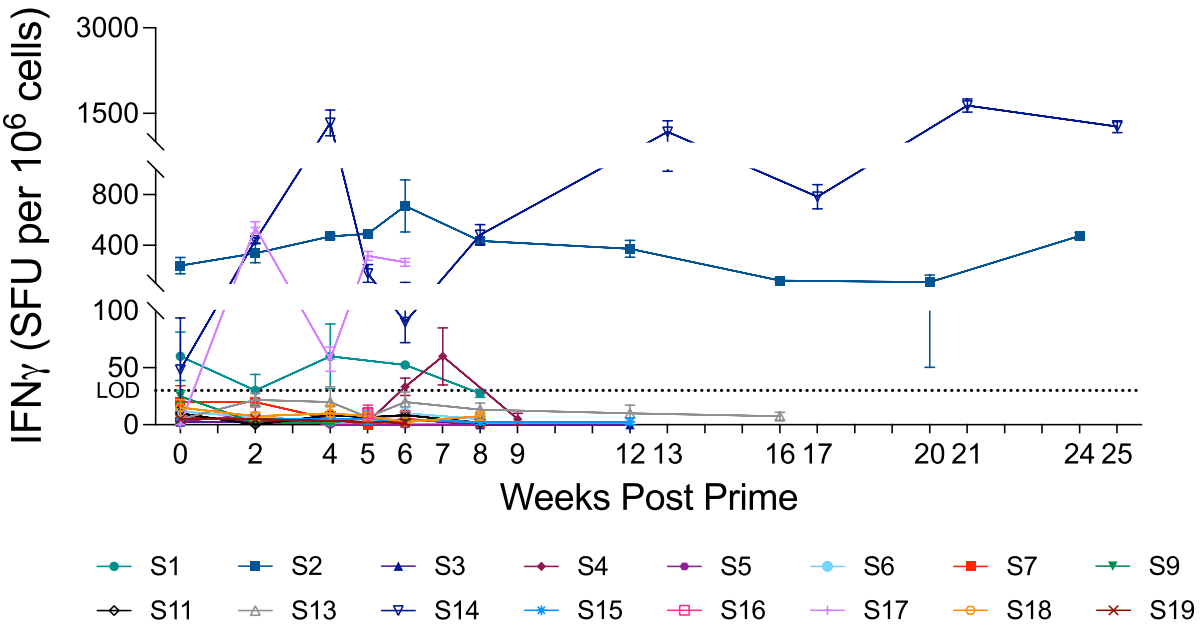

Extended Data Fig. 4 | Tumor neoantigen specific T cell responses measured by ex vivo IFNγ ELISpot in PBMCs at baseline and at various timepoints post ChAd68 prime for each patient. *n* = 16 patients (S8 and S10 not tested by ex vivo ELISpot). LOD 30. Data presented as mean SFU/10^6 cells ± s.d. for 2 – 3 technical replicates per sample.

https://doi.org/10.1038/s41591-024-02851-9

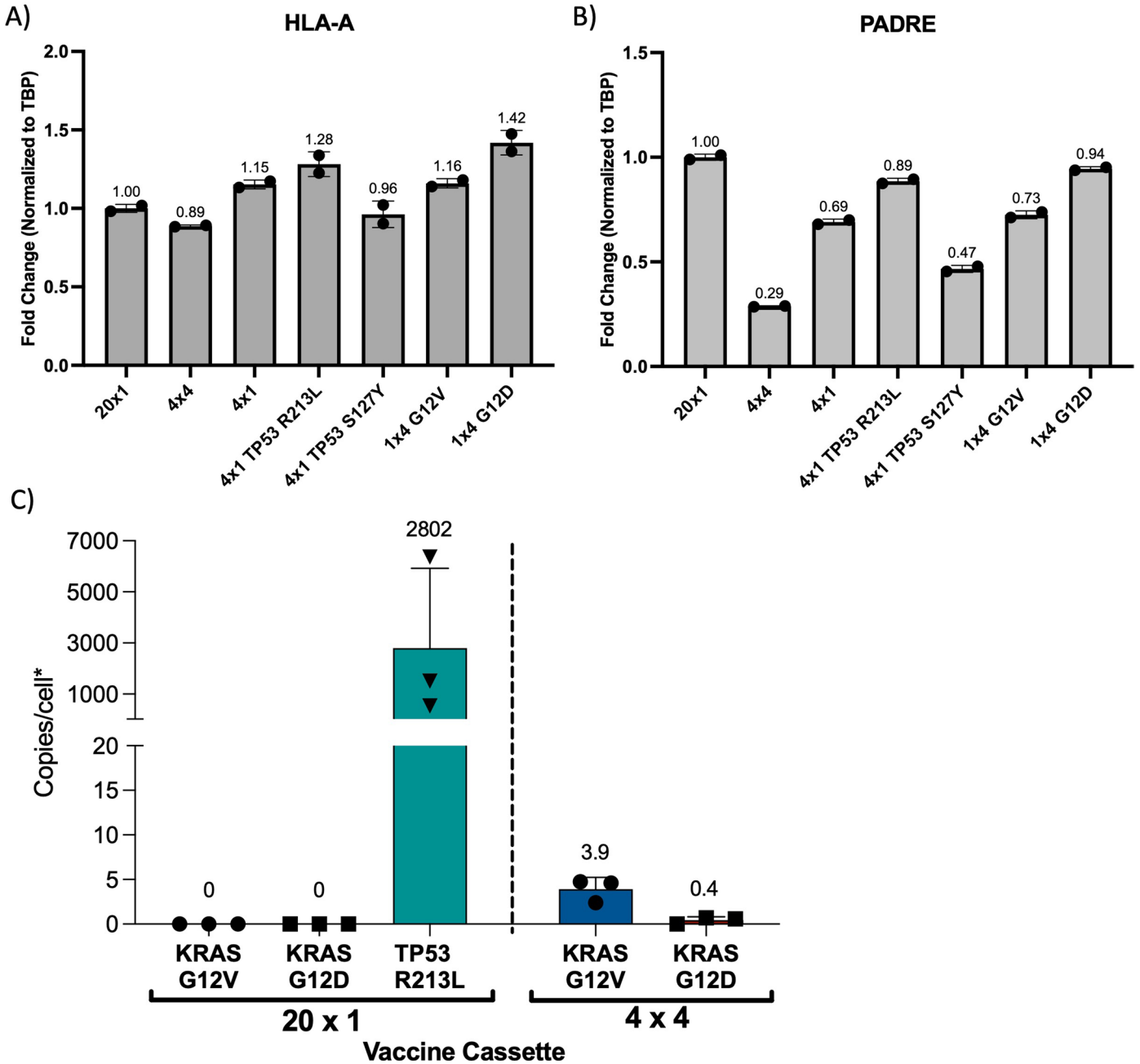

Extended Data Fig. 5 | Expression levels in cell lines used for mass spectrometry and analysis of HLA-A*02 expressing cell lines. Transcript levels of HLA-A (A) and PADRE (Pan HLA DR epitope presented at the c-terminal of each epitope cassette) (B) measured by comparative real-time PCR in engineered K562 monoallelic HLA-A*11:01 cell lines expressing different formats of epitope cassettes. Fold-change normalized to *TBP* housekeeping gene. Mean fold-change ± s.d. are shown for 2 technical replicates. Mean values annotated above bars. (C) Target density of KRAS and TP53 epitopes detected by mass spectrometry in HLA-A*02:01 monoallelic cell lines. TP53-R213L measured in A*02:01 K562 lines transduced with the SLATEv1 cassette (20×1, 20 unique epitopes with 1 copy each) using cassettes with doxycycline-induced expression or zeocin selection. Data presented as mean copies/cell ± s.d. of 3 independent experiments, mean value annotated. No KRAS antigens were detected in 20×1, but very low levels of KRAS G12V and G12D were detected in 3 A*02:01 K562 lines transduced with SLATE 4×4 cassettes (4 unique KRAS epitopes with 4 copies each in cassettes engineered with either blastocidin or hygromycin selection) which have no TP53 epitopes included. *Copies/cell are reported as measured by relative response of endogenous peptide to stable isotopic labeled synthetic peptide added to isolated sample immunopeptides immediately before mass spectrometry analysis, then adjusted for an average 9% pHLA process recovery.

https://doi.org/10.1038/s41591-024-02851-9

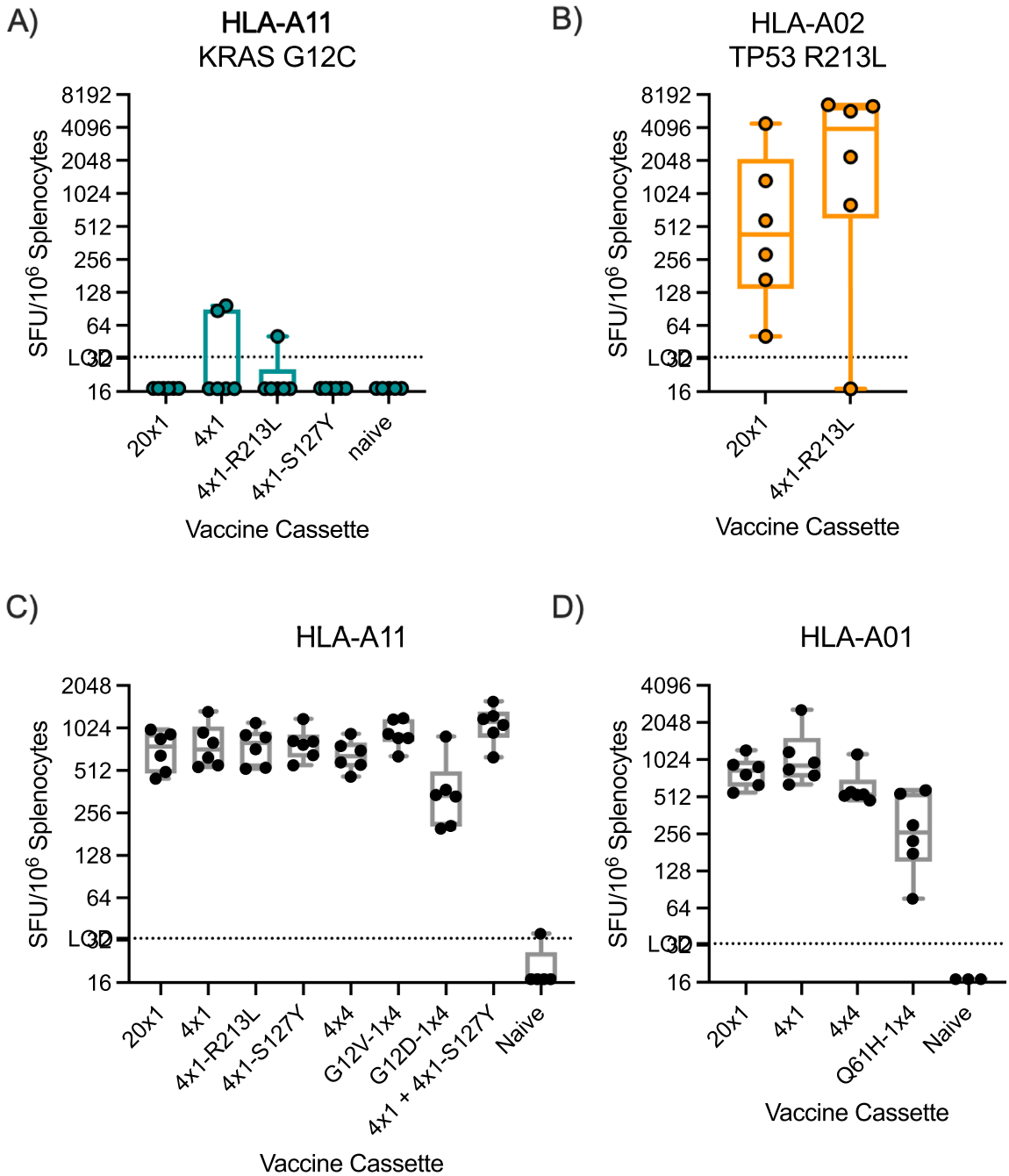

Extended Data Fig. 6 | Immunogenicity of vaccines assessed in HLA transgenic mice. (A) Antigen-specific T cell response assessed in splenocytes of HLA-A*11 transgenic mice (n = 6/group) 2 weeks post intramuscular immunization with the specified ChAd vaccine (5×10^{10} VP each) by IFNγ ELISpot following overnight stimulation with the KRAS G12C minimal epitope peptide (VVVGACGVGK). (B) Antigen-specific T cell response assessed in splenocytes of HLA-A*02 transgenic mice (n = 6/group) 2 weeks post intramuscular immunization with the specified ChAd vaccine (5×10^{10} VP each) by IFNγ ELISpot following overnight stimulation with the TP53-R213L peptide pool containing all possible 8 – 11mer epitopes spanning the neoantigen 25mer. (C-D) Antigen-specific T cell response assessed in splenocytes of HLA-A*11 (C) or HLA-A*01 (D) transgenic mice (n = 6/group) 2 weeks post intramuscular immunization with the specified ChAd vaccine (5×10^{10} VP each) by IFNγ ELISpot following overnight stimulation with the PADRE peptide. Data from same experiments shown in Fig. 4, representative data from 2 studies. (A-D) Box and whiskers represent IQR and range, line is median, log2 scale. LOD 33, values < LOD set to one-half LOD.

https://doi.org/10.1038/s41591-024-02851-9

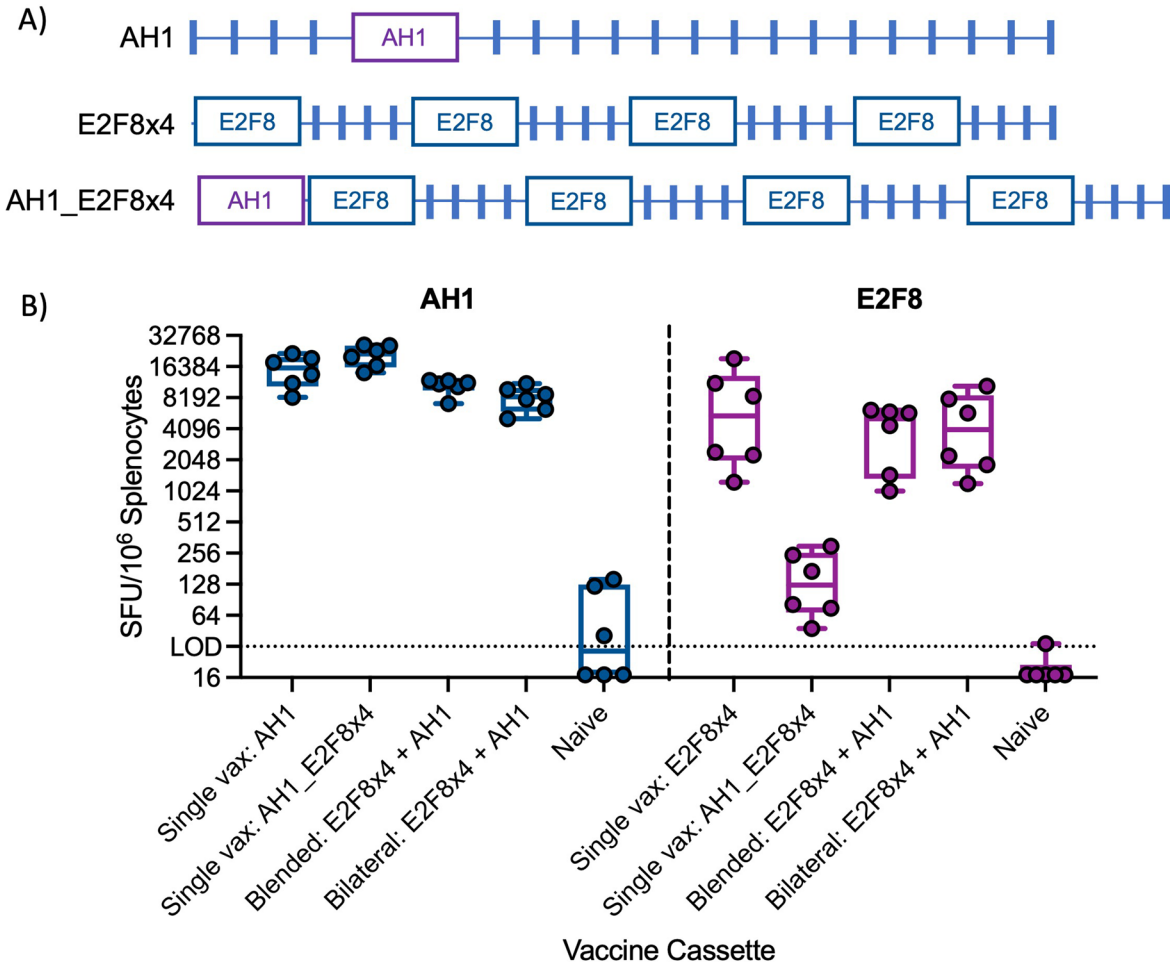

Extended Data Fig. 7 | Expression of immunodominant AH1 epitope on the same vaccine cassette leads to decreased immune response to the E2F8 sub-dominant epitope, rescued by delivery of both epitopes in different vaccines. (A) Design of vaccine epitope cassettes evaluated for immunogenicity in Balb/c mice. Boxes represent epitopes for which immune data is presented, lines represent other epitopes. (B) Antigen-specific T cell response assessed in splenocytes of Balb/c mice (n = 6/group) 2 weeks post intramuscular immunization with the specified ChAd vaccine (5×10^9 VP each) by IFNγ ELISpot following overnight stimulation with the specified peptide. Single vaccines were administered bilaterally, 2.5×10^9 vp per leg, for a total dose of 5×10^9 VP. For the blended approach vaccines were combined in a single syringe and then delivered bilaterally (5×10^9 VP each vaccine, 1×10^{10} VP total), for the bilateral approach mice received 1×10^{10} VP of ChAd (5×10^9 VP of E2F8×4 in the left tibialis anterior (TA) and 5×10^9 VP of AH1 in the right TA). Box and whiskers represent IQR and range, line is median, log2 scale. LOD 33, values < LOD set to one-half LOD.

https://doi.org/10.1038/s41591-024-02851-9

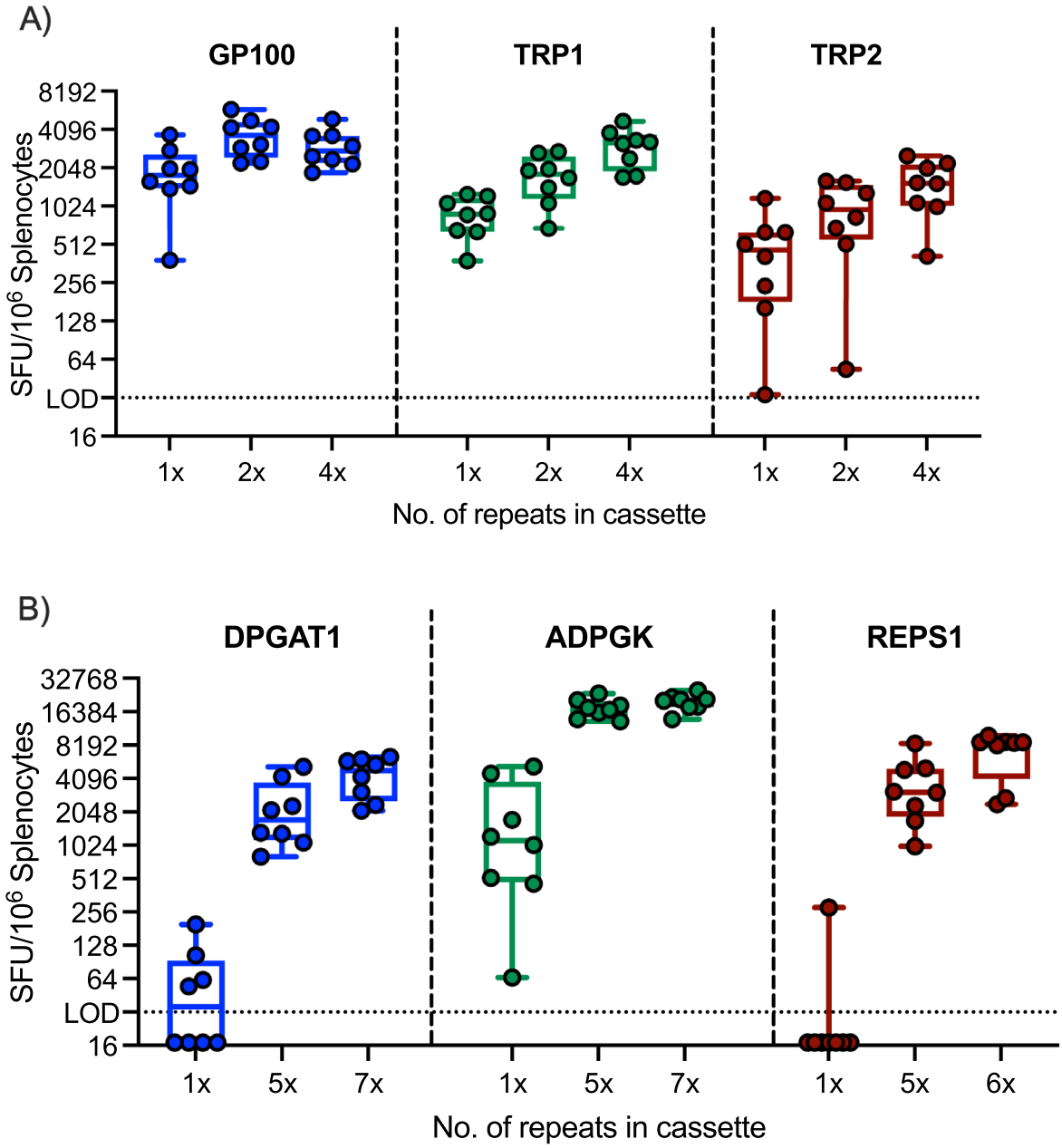

Extended Data Fig. 8 | Antigen repetition within vaccine expression cassette leads to increased antigen-specific T cell responses. (A-B) Antigen-specific T cell response assessed in splenocytes of C57BL6 mice (n = 8/group) 2 weeks post immunization. IFNγ ELISpot following overnight stimulation with the specified peptide. Box and whiskers represent IQR and range, line is median, log2 scale. LOD = 33, values < LOD set to ½ LOD. (A) Mice immunized with 10 µg samRNA expressing a vaccine cassette encoding 20 mouse epitopes (1x), 10 epitopes repeated twice (2x), or 5 epitopes repeated 4 times (4x). Data from 3 H2-Kb restricted epitopes derived from B16 tumor mouse model shown. (B) Mice immunized with $1x10^9$ VP ChAd vaccine encoding 20 epitopes with no repeats (20x1), 3 epitopes repeated 5 times (5x), or 3 epitopes repeated 6-7 times (6x or 7x). Data from 3 H2-Kb restricted epitopes derived from MC38 tumor mouse model shown.

https://doi.org/10.1038/s41591-024-02851-9

Extended Data Table 1 | Shared neoantigens encoded by SLATEv1 vaccine cassette

Neoantigen mutation	Mutation	Mass-Spec Validated HLA Class I Alleles	Predicted HLA Class I Alleles
1	KRAS_G13D	A1101, A6801	C0802
2	KRAS_Q61K	A0101	–
3	TP53_R249M	-	B3512, B3503, B3501
4	CTNNB1_S45P	A0301, A1101	A0302, A6801
5	CTNNB1_S45F	A1101, A6801	A0301
6	ERBB2_Y772_A775dup	A0101	B1801
7	KRAS_G12D[a]	A0201, A0301, A1101, A6801, B0702, C0304,C0802[b]	-
8	KRAS_Q61R	A0101	-
9	CTNNB1_T41A	A0301, A1101, C0304	A0302, B1510, C0303
10	TP53_K132N	A2402	A2301
11	KRAS_G12A	A0301, A1101, A6801	-
12	KRAS_Q61L	A0101, B4405	-
13	TP53_R213L	A0201, C0304	A0207, C0802
14	BRAF_G466V	A0301, A1101	B1501, B1503
15	KRAS_G12V[a]	A0201, A0301, A1101, A6801, B0702, C0102, C0304	A0302
16	KRAS_Q61H[a]	A0101	-
17	CTNNB1_S37F	A0101, A0201	A2301, A2402, B1510, B3906, C0501, C1402, C1403
18	TP53_S127Y	A0301, A1101	-
19	TP53_K132E	-	A2402, C1403, A2301
20	KRAS_G12C[a]	A0201, A0301, A1101, A6801, B0702, C0304	-

[a]Shared neoantigens included in SLATE-KRAS vaccine cassette. [b]Epitope validation in HLA-C*08:02 published for an adoptive T-cell therapy treated patient[13].

https://doi.org/10.1038/s41591-024-02851-9

Extended Data Table 2 | Phase I patient demographics

Dose Level (DL)[a]	Patient ID	Tumor Type	Tumor mutation	Matched HLA allele	Number of prior lines of therapy	Time to first GRT-C903 since cancer diagnosis (Month)	Sex[b]	Race[b]	Age (years)	ECOG	BOR[c]	PFS (months)[d]	OS (months)[e]	Reason for treatment discontinuation
DL1	S1	NSCLC	KRAS G12C	A*02:01	3	14.3	M	Black or AA	67	1	PD	1.9	3.8	PD
DL1	S2	NSCLC	KRAS G12C	A*02:01	3	29.9	F	White	83	1	SD	9.5	9.5	PHYSICIAN DECISION
DL2	S3	NSCLC	KRAS G12C	A*02:01	1	11.9	M	White	64	1	SD	24.8	37.1+	COMPLETED
DL2	S4	CRC	KRAS Q61H	A*01:01	2	22	F	White	33	1	PD	1.4	3.4	PD
DL2	S5	PDA	KRAS G12D	A*11:01	1	46.6	M	White	67	1	PD	1.4	2.6	PD
DL2	S6	NSCLC	KRAS G12D	A*03:01; A*11:01	1	6.5	M	White	78	0	PD	1.9	3.6	PD
DL3	S7	CRC	KRAS Q61H	A*01:01	2	54.5	F	White	62	1	SD	3.6+	3.6+	WITHDRAWAL BY SUBJECT
DL3	S8	Ovarian adenocarcinoma	KRAS G12V	A*11:01	3	40.5	F	White	53	0	PD	1.9	28.2	PD
DL3	S9	PDA	KRAS G12V	A*03:01	3	34.2	F	White	60	1	PD	1.7	6.5	PD
DL3	S10	NSCLC	KRAS Q61H	A*01:01	1	12.8	F	White	67	1	SD	21.2	21.2	WITHDRAWAL BY SUBJECT
DL3	S11	PDA	KRAS G12V	A*11:01	1	6.1	M	Asian	48	1	SD	3.9	6.8	PD
DL3	S12	CRC	TP53 R213L	A*02:01	1	18.8	F	White	75	1	PD	0.7	4.7	PD
DL4	S13	CRC	KRAS G12V	A*11:01	2	58.7	F	White	43	1	PD	1.8	7	PD
DL4	S14	NSCLC	KRAS G12D	A*11:01	1	25.9	F	White	79	1	SD	23.8	23.8	WITHDRAWAL BY SUBJECT
DL4	S15	Pancreatobiliary adenocarcinoma	KRAS G12V	A*11:01	3	34	F	Asian	39	1	SD	3.6	7.9	PD
DL4	S16	PDA	KRAS G12V	A*03:01	3	58	F	White	61	1	SD	3.4	7.9	PD
DL4	S17	CRC	KRAS G12D	A*11:01	1	3.7	M	White	54	0	PD	1.9	8.4	PD
DL4	S18	CRC	KRAS G13D	C*08:02	1	21.1	F	White	35	1	PD	1.8	10.9	PD
DL4	S19	PDA	KRAS G12D	A*03:01; C*08:02	1	31.4	M	White	61	1	PD	1	16.7	PD

CRC: Colorectal Cancer, NSCLC: Non-Small Cell Lung Cancer, PDA: pancreatic ductal adenocarcinoma. [a] Dose Level 1=GRT-C903/GRT-R904 30 µg + nivolumab; Dose Level 2=GRT-C903/GRT-R904 30 µg + nivolumab + SC ipilimumab; Dose Level 3=GRT-C903/GRT-R904 100 µg + nivolumab + SC ipilimumab; Dose Level 4=GRT-C903/GRT-R904 300 µg + nivolumab + SC ipilimumab. [b] Sex and Race self-reported. M: Male, F: Female, AA: African American. All patients reported as "Not Hispanic or Latino". [c] BOR: Best of response as per RECIST v 1.1; PD: progressive disease, SD: stable disease. [d] PFS: Progression Free Survival, time from the first dose with GRT-C903 to the earliest date of PD or death by any cause. [e] OS: Overall Survival, time to death or last contact from the 1st study treatment. + denotes censored subjects (alive and without PD at last contact for PFS and alive at last contact for OS).

nature portfolio

Corresponding author(s): Karin Jooss

Last updated by author(s): Jan 25, 2024

Reporting Summary

Nature Portfolio wishes to improve the reproducibility of the work that we publish. This form provides structure for consistency and transparency in reporting. For further information on Nature Portfolio policies, see our Editorial Policies and the Editorial Policy Checklist.

Statistics

For all statistical analyses, confirm that the following items are present in the figure legend, table legend, main text, or Methods section.

n/a	Confirmed	
☐	☒	The exact sample size (*n*) for each experimental group/condition, given as a discrete number and unit of measurement
☐	☒	A statement on whether measurements were taken from distinct samples or whether the same sample was measured repeatedly
☐	☒	The statistical test(s) used AND whether they are one- or two-sided *Only common tests should be described solely by name; describe more complex techniques in the Methods section.*
☒	☐	A description of all covariates tested
☒	☐	A description of any assumptions or corrections, such as tests of normality and adjustment for multiple comparisons
☐	☒	A full description of the statistical parameters including central tendency (e.g. means) or other basic estimates (e.g. regression coefficient) AND variation (e.g. standard deviation) or associated estimates of uncertainty (e.g. confidence intervals)
☐	☒	For null hypothesis testing, the test statistic (e.g. *F*, *t*, *r*) with confidence intervals, effect sizes, degrees of freedom and *P* value noted *Give P values as exact values whenever suitable.*
☒	☐	For Bayesian analysis, information on the choice of priors and Markov chain Monte Carlo settings
☒	☐	For hierarchical and complex designs, identification of the appropriate level for tests and full reporting of outcomes
☒	☐	Estimates of effect sizes (e.g. Cohen's *d*, Pearson's *r*), indicating how they were calculated

Our web collection on statistics for biologists contains articles on many of the points above.

Software and code

Policy information about availability of computer code

Data collection	AID ELISpot reader software, vSpot 7.0 (Autoimmun Diagnostika) NovaSeq Control Software 1.7 (Illlumina) Orbitrap Fusion Lumos Tribrid Control Software 4.0 (Thermo Fisher Scientific, Inc.) Xcalibur 4.6 (Thermo Fisher Scientific, Inc.)
Data analysis	GraphPad Prism (GraphPad Software LLC, Version 9.5.1.) Skyline Daily 23.0.9.157 (University of Washington, MacCoss Lab). ProteomicsDB Universal Spectrum Explorer (https://www.proteomicsdb.org/use/) fgbio 0.7.0 (cfDNA pipeline) and 2.0.2 (HLA analysis) (github, http://fulcrumgenomics.github.io/fgbio/tools/latest/) FreeBayes v1.0.0 (http://arxiv.org/abs/1207.3907, https://github.com/freebayes/freebayes) Vardictjava 1.6.0 (https://github.com/AstraZeneca-NGS/VarDictJava) bwa v0.7.13 (http://arxiv.org/abs/1303.3997, http://bio-bwa.sourceforge.net/) Picard v2.7.1 (github, https://broadinstitute.github.io/picard/) Genome Analysis Toolkit (GATK) 4.2.6.1. https://gatk.broadinstitute.org/hc/en-us CFX Manager v3.1 (BioRad) SAS 9.4

For manuscripts utilizing custom algorithms or software that are central to the research but not yet described in published literature, software must be made available to editors and reviewers. We strongly encourage code deposition in a community repository (e.g. GitHub). See the Nature Portfolio guidelines for submitting code & software for further information.

Data

Policy information about availability of data

All manuscripts must include a data availability statement. This statement should provide the following information, where applicable:

- Accession codes, unique identifiers, or web links for publicly available datasets
- A description of any restrictions on data availability
- For clinical datasets or third party data, please ensure that the statement adheres to our policy

De-identified individual participant clinical data that underlie the results reported in this article are available for transfer. Interested investigators can obtain and certify the data transfer agreement (DTA) and submit requests to the principal investigator K.J. Investigators and institutions who consent to the terms of the DTA form, including, but not limited to, the use of these data for the purpose of a specific project and only for research purposes, and to protect the confidentiality of the data and limit the possibility of identification of participants in any way whatsoever for the duration of the agreement, will be granted access. Gritstone will then facilitate the transfer of the requested de-identified data. This mechanism is expected to be via a Gritstone Secure File Transfer Service, but Gritstone reserves the right to change the specific transfer method at any time, provided appropriate levels of access authorization and control can be maintained. Source data are provided with this paper. Epitope selection utilized a previously published algorithm (Bulik-Sullivan et al., Nature Biotechnology, 2018).

Research involving human participants, their data, or biological material

Policy information about studies with human participants or human data. See also policy information about sex, gender (identity/presentation), and sexual orientation and race, ethnicity and racism.

Reporting on sex and gender	Due to the relatively small number of patients in this study, no sex- or gender-based stratifications were considered. Sex was determined by self-report and has been reported for each patient. 12 female and 7 male patients were included. For preclinical animal studies, only female mice were used.
Reporting on race, ethnicity, or other socially relevant groupings	Reporting of race, ethnicity and socially relevant grouping was based on collected demographics and no further stratification analysis was conducted due to size of the trial.
Population characteristics	Patients with advanced or metastatic non-small cell lung cancer, pancreatic ductal adenocarcinoma, microsatellite stable colorectal cancer, or any other solid tumors with the relevant mutation (where the patient has experienced disease progression with all available therapies known to confer clinical benefit) who are ≥ 18 years of age.
Recruitment	Patients were recruited at selected clinical sites across the United States of America. Patient recruitment occurred via site staff presenting the study to patients under their medical care. Elibility criteria selected for patients with tumors known to have the specified mutations who had received or were receiving standard of care therapy for their tumor. Patients were required to be in sufficiently well to participate in a clinical study (eg, good performance status). Therefore this study population may not reflect patiens with cancer whose activities of daily life are severely compromised and this is reflected in the inclusion criteria consistent with first-in-human clinical oncology studies.
Ethics oversight	The protocol was reviewed and approved by an institutional review board (IRB) at each participating clinical site.

Note that full information on the approval of the study protocol must also be provided in the manuscript.

Field-specific reporting

Please select the one below that is the best fit for your research. If you are not sure, read the appropriate sections before making your selection.

☒ Life sciences ☐ Behavioural & social sciences ☐ Ecological, evolutionary & environmental sciences

For a reference copy of the document with all sections, see nature.com/documents/nr-reporting-summary-flat.pdf

Life sciences study design

All studies must disclose on these points even when the disclosure is negative.

Sample size	19 patients. For the clinical study, the sample size is not driven by a statistical power due to the nature of an adaptive dose escalation method. Phase 1 sample size was range from 11 to 24 patients based on the adaptive mTPI-2 design. For mouse studies: n = 6 mice per group. This number was selected based on previous observations of biological variability in immune responses across animals, as the minimal number required to ensure that differences in responses elicited by the different vaccines could be determined.
Data exclusions	Patients S3, S7, S8, S12, S14, S15, and S19 were excluded from ctDNA analysis due to no detectable ctDNA levels at baseline. Immune analysis was not performed for patient S12 because no post-treatment samples were collected. For immune analysis: patients S8 and S10 were only assessed by IVS/ELISpot and not by ex vivo ELISpot. For patient S8 there was only one post-treatment sample collected. Patient S18 was assessed by ex vivo ELISpot, but not IVS/ELISpot, due to insufficient sample. Patients S4, S7, S10 and S18 were not assessed for TP53 response due to no HLA match, S8 and S19 were not tested due to insufficient sample. For some patients, baseline samples with insufficient volume were only assessed by one assay (either IVS/ELISpot or ex vivo ELISpot), these are annotated as N.T. (not tested) in figures.

Replication	All assays were performed with technical replicates. Immune assays were only repeated on clinical samples if assay control criteria failed. Mouse studies were repeated 2 - 3 times, as noted in the figure legends.
Randomization	No randomization was performed for this first-in-human phase 1/2 study.
Blinding	Investigators were not blinded to study treatment as this was a single arm, first-in-human study designed to assess the safety and tolerability of this vaccine regimen.

Reporting for specific materials, systems and methods

We require information from authors about some types of materials, experimental systems and methods used in many studies. Here, indicate whether each material, system or method listed is relevant to your study. If you are not sure if a list item applies to your research, read the appropriate section before selecting a response.

Materials & experimental systems

n/a	Involved in the study
☒	☐ Antibodies
☐	☒ Eukaryotic cell lines
☒	☐ Palaeontology and archaeology
☐	☒ Animals and other organisms
☐	☒ Clinical data
☒	☐ Dual use research of concern
☒	☐ Plants

Methods

n/a	Involved in the study
☒	☐ ChIP-seq
☒	☐ Flow cytometry
☒	☐ MRI-based neuroimaging

Eukaryotic cell lines

Policy information about cell lines and Sex and Gender in Research

Cell line source(s)	K562 - ATCC CCL-243 293T - ATCC CRL-3216 293F - Thermo, #11625019
Authentication	Cell lines were purchased from ATCC or Thermo and were authenticated by the vendor. No further authentication was performed.
Mycoplasma contamination	Cells were confirmed negative for mycoplasma
Commonly misidentified lines (See ICLAC register)	None

Animals and other research organisms

Policy information about studies involving animals; ARRIVE guidelines recommended for reporting animal research, and Sex and Gender in Research

Laboratory animals	Mouse (mus musculus): HLA-A11:01 (#9660), HLA-A2:01 (#9659), and HLA-A1:01 (#9662); all transgenic mice were obtained from Taconic and are on a CB6F1 background. C57BL6 mice (Envigo) were used as unvaccinated controls and for evaluation of mouse antigen vaccines. All mice were female, > 6 weeks old and < 1 year old.
Wild animals	Study did not involve wild animals
Reporting on sex	Only female mice were used.
Field-collected samples	Study did not involve field-collected samples
Ethics oversight	Mouse studies were approved by Murigenics IACUC (Vallejo, CA).

Note that full information on the approval of the study protocol must also be provided in the manuscript.

Clinical data

Policy information about clinical studies

All manuscripts should comply with the ICMJE guidelines for publication of clinical research and a completed CONSORT checklist must be included with all submissions.

Clinical trial registration	NCT03953235

Study protocol	Study protocol is available as part of the supplemental information submitted with the manuscript.
Data collection	Clinical data was collected in an electronic data capture system database based on case report forms. Patients were enrolled from July 18, 2019 to March 12, 2020 for phase 1 portion of the study. Immunogenicity data were generated and analyzed by the study sponsor using patient's peripheral blood mononuclear cells.
Outcomes	The primary endpoints for Phase 1 were safety and tolerability of the vaccine regimen and to define the recommended Phase 2 dose. The secondary endpoints for Phase 1 included immunogenicity, objective response rate (ORR), progression free survival (PFS) and overall survival (OS). Exploratory endpoints included analysis of biomarkers, such as circulating tumor DNA. Adverse events (AEs) were coded using the Medical Dictionary for Regulatory Activities (MedDRA) v 21.1. Common Terminology Criteria for Adverse Events (CTCAE) were used to grade the severity of AEs. Treatment-emergent AE (TEAE) were defined as any AE with onset after the administration of study medication through 100 days post treatment or initiation of alternative anti-cancer therapy, whichever occurred first or any event that was present at baseline but worsened in intensity or was subsequently considered drug-related by the investigator through the end of the study. ORR was based on RECIST v. 1.1. BOR was defined as the best response recorded from the study treatment start until disease progression or death whichever comes earlier. PFS was defined as the date of first dose with GRT-C903 to the earliest date of progression or death by any cause (in the absence of progression). OS was measured from the date of the first dose of GRT-C903 to the date of death by any cause. OS time for patients alive by the end of study was censored at the last date that patient surviving status is known. The median PFS and OS were estimated by Kaplan-Meier method and the corresponding two-sided 95% confidence intervals were calculated according to Brookmeyer and Crowley method. Immunogenicity was assessed by IFNgamma ELISpot analysis of PBMCs.